

On Turbulent Particle Pair Diffusion

NADEEM A. MALIK [†]

Department of Mathematics and Statistics, King Fahd University of Petroleum and Minerals,
P.O. Box 5046, Dhahran 31261, Kingdom of Saudi Arabia

(Received ?; revised ?; accepted ?. - To be entered by editorial office)

Richardson's theory of turbulent particle pair diffusion [Richardson, L. F. Proc. Roy. Soc. Lond. A 100, 709737, 1926], based upon observational data, is equivalent to a locality hypothesis in which the turbulent pair diffusivity (K) scales with the pair separation (σ_l) with a 4/3-power law, $K \sim \sigma_l^{4/3}$. Here, a reappraisal of the 1926 dataset reveals that one of the data-points is from a molecular diffusion context; the remaining data from geophysical turbulence display an unequivocal non-local scaling, $K \sim \sigma_l^{1.564}$. Consequently, the foundations of pair diffusion theory have been re-examined, leading to a new theory based upon the principle that both local and non-local diffusional processes govern pair diffusion in homogeneous turbulence. Through a novel mathematical approach the theory is developed in the context of generalised power law energy spectra, $E(k) \sim k^{-p}$ for $1 < p \leq 3$, over extended inertial subranges. The theory predicts the scaling, $K(p) \sim \sigma_l^{\gamma_p}$, with γ_p intermediate between the purely local and the purely non-local scalings, i.e. $(1+p)/2 < \gamma_p \leq 2$. A Lagrangian diffusion model, Kinematic Simulations [Kraichnan, R. H., Phys. Fluids 13, 22-31, 1970; Fung et al., J. Fluid Mech. 236, 281-318, 1992], is used to examine the predictions of the new theory all of which are confirmed. The simulations produce the scalings, $K \sim \sigma_l^{1.545}$ to $\sim \sigma_l^{1.570}$, in the accepted range of intermittent turbulence spectra, $E(k) \sim k^{-1.72}$ to $\sim k^{-1.74}$, in close agreement with the revised 1926 dataset.

Key words: Turbulence, pair diffusion, Richardson, non-local, mathematical foundations, simulation

1. Introduction

Turbulent transport and mixing play an essential role in many natural and industrial processes Shraiman (2000), in cloud formation Vaillancourt & Yau (2000), in chemical reactors and combustion systems Pope (1994), and atmospheric and oceanographic turbulence determines the spread of pollutants and biological agents in geophysical flows Huber et al. (2001), Berloff et al. (2002), Wolf et al. (2004), Joergensen et al. (2005). Concentration fluctuations are often of great importance in such systems and this is related to the separation of nearby fluid particles; turbulent pair diffusion therefore plays a critical role in such systems. The idea of locality has been fundamental to the theory of turbulent particle pair diffusion since Richardson's pioneering paper, Richardson (1926),

[†] Email: namalik@kfupm.edu.sa, and nadeem_malik@cantab.net

which established turbulent pair diffusion as an important scientific discipline and laid the foundations for a theory of how ensembles of pairs of fluid particles (tracers) initially close together move apart due to the effects of atmospheric winds and turbulence. Richardson argued that as particle pairs separate the rate at which they move apart is affected mostly by eddies of the same scale as the separation distance itself this is the basis of the locality hypothesis. Richardson was also motivated by a desire to bring molecular and turbulent pair diffusional processes into a unified picture through the use of a single non-Fickian diffusion equation with scale dependent diffusivity, $K(r)$, where r is the pair separation variable. Assuming homogeneous isotropic turbulence, Richardson posed the problem in 3D in terms of the probability density function (pdf) of the pair separation, $q = q(r, t)$, and assuming the normalization, $\int_0^\infty 4\pi r^2 q(r, t) dr = 1$, he suggested the following diffusion equation to describe q ,

$$\frac{\partial q}{\partial t} = \frac{1}{r^2} \frac{\partial}{\partial r} \left(r^2 K(r) \frac{\partial q}{\partial r} \right) \quad (1.1)$$

The scaling of the pair diffusivity K with the pair separation and what it means for the pair diffusion process is of paramount importance. From observational data of turbulent pair diffusivities collected from different sources, Richardson assumed an approximate fit to the data namely, $K \sim l^{4/3}$. This is equivalent to $\langle l^2 \rangle \sim t^3$, Obukhov (1941), Batchelor (1952), often referred to as the Richardson-Obukov t^3 -regime. $l(t)$ is the pair separation, t is the time, and the angled brackets is the ensemble average over particle pairs.

It is no longer believed that it is possible to unify molecular and turbulent diffusional processes because their physics are fundamentally different; Brownian motion characterizes molecular diffusion, while convective gusts of winds that increase the pair separation in surges characterizes turbulent diffusion Wilkins (1958), Fung et al. (1992), Virant & Dracos (1997). Nevertheless, the idea of a scale dependent turbulent diffusivity has survived.

Richardson's assumed 4/3-scaling law is equivalent to a locality hypothesis, according to which for asymptotically large Reynolds number only the energy in eddies whose size is of a similar scale to the pair separation inside the inertial subrange is effective in further increasing the pair separation. Furthermore, Richardson's scaling for the pair diffusion is consistent with Kolmogorov (1941), (K41); this can be seen from the form of the turbulence energy spectrum in the inertial subrange which is, $E(1/l) \sim \varepsilon^{2/3} (1/l)^{-5/3}$, from which it follows that the pair diffusivity depends only upon l and ε (the rate of kinetic energy dissipation per unit mass). This leads directly to the locality scaling, $K \sim \varepsilon^{1/3} l^{4/3}$. It is usual to evaluate K at typical values of, l , namely at $\sigma_l = \sqrt{\langle l^2 \rangle}$, so this scaling is replaced by, $K \sim \varepsilon^{1/3} \sigma_l^{4/3}$. The requirement of large Reynolds number, $Re \rightarrow \infty$, implies that this scaling is true only inside an asymptotically infinite inertial subrange, $\eta \ll \sigma_l \ll L$, where $L/\eta \rightarrow \infty$, and η is the Kolmogorov micro-scale and L is a scale characteristic of energy containing eddies, typically the integral length scale, or the Taylor length scale. In this limit, the pair separation is initially zero, $l \rightarrow 0$, as $t \rightarrow 0$.

For finite inertial subrange, there are infra-red and ultra-violet boundary corrections so the inertial subrange still has to be very large in order to avoid these effects and to observe inertial subrange scaling in the pair diffusion. With the 4/3-scaling for K , an explicit solution for equation (1.1) for diffusion from a point source with boundary

conditions $q(0, t) = q(\infty, t) = 0$, can be derived,

$$q(r, t) = \frac{429}{70} \sqrt{\frac{143}{2}} \left(\frac{1}{\pi \langle r^2(t) \rangle} \right)^{3/2} \exp \left(- \left(\frac{1287}{8 \langle r^2(t) \rangle} \right)^{1/3} \right) \quad (1.2)$$

Turbulence is both scale dependent and time correlated (non-Markovian), and it is not clear whether the pdf in equation (1.2), which describes a local and Markovian process, can accurately represent the turbulent pair diffusion process. Attempts have been made to derive alternative non-Markovian models for pair diffusion, Falkovich et al. (2001), Eyink & Benveniste (2013), and this remains a subject of ongoing scientific research. However, this does not affect Richardson's hypothesis of scale dependent diffusivity, which is the main focus of this study.

It is possible to generalize the scaling for the pair diffusivity to be time dependent and still be consistent with K41 and with locality, Klafter et al. (1987), Salazar & Collins (2009), such that,

$$K \sim \varepsilon^a t^b l^c \quad (1.3)$$

for some a, b , and c . Dimensional consistency then gives, $2a + c = 2$ and $3a - b = 1$, which leads to $a = 1/3 - b/3$, and $c = 4/3 - 2b/3$. Thus we obtain,

$$K \sim \varepsilon^{(1/3-b/3)} t^b l^{(4/3-2b/3)} \quad (1.4)$$

If the further constraint $2b + 3c = 4$ is satisfied, then this yields, $\langle l^2 \rangle \sim t^3$. Thus, a t^3 -regime is not a unique signature for Richardson's 4/3-scaling for the pair diffusivity. However, a time dependent pair diffusivity is hard to justify physically if we assume steady state equilibrium turbulence, because a time dependent diffusivity implies, for $b > 0$ that the pair diffusivity at the same separation is ever increasing in time without limit, or for $b < 0$ that the pair diffusivity approaches zero with time and the separation process effectively stops. Both cases seem unlikely, and in the ensuing we will restrict the discussion to steady state equilibrium turbulence and consider only the case, $b = 0$. However, it is worth remarking that time-dependent diffusivities like equation (1.3) may exist in the context of non-equilibrium turbulence.

The main aims of this research are two-fold. Firstly, to re-examine the body of evidence available on turbulent pair diffusion especially, if any, from large scale turbulence containing large inertial subranges, Section 2. Particular attention is focussed upon a reappraisal of Richardson's original 1926 dataset, Section 3. Secondly, based upon these findings, a new theory that does not *a priori* make the assumption of locality is constructed from which new scaling laws for the pair diffusivity is derived through a novel mathematical method, and compared to the reappraised 1926 dataset, in Section 4. Finally, a Lagrangian diffusion model is used to examine the new theory and the results from the simulations are found to agree closely with the 1926 dataset and with the predictions of the new theory, Section 5. We discuss the significance of these findings and draw conclusions in Section 6.

2. What is the evidence for locality?

Although the general consensus among scientists in the field at the current time is that the collection of observational data, experimental data, and Direct Numerical Simulation, suggests a convergence towards a Richard-Obukov locality scaling, the relatively low Reynolds numbers in the experiments and DNS, and the high error levels, and other assumptions made in collecting the data means that this is by no means a forgone conclusion. As noted by Salazar & Collins (2009), " .. there has not been an experiment that has unequivocally confirmed R-O scaling over a broad-enough range of time and with sufficient accuracy." It is not known precisely what size of the inertial subrange is required to observe unequivocally the pair diffusion scaling, but it is widely assumed to be about at least four orders of magnitude or more. Only geophysical turbulent flows, such as in the atmosphere and in the oceans, can produce such extended inertial subranges.

A number of claims of observing locality scaling, including the existence of an approximate t^3 -regime in geophysical flows, have been made by Tatarski (1960), Wilkins (1958), Sullivan (1971), and Morel & Larchaveque (1974). More recent observations include Julian et al. (1977) in the atmosphere, and LaCasce & Ohlmann (2003), and Ollitrault et al. (2005) in the oceans. But high error levels and other assumptions (such as two-dimensionality) made in these observations means that decisive conclusions cannot be drawn from them regarding pair diffusion theories.

Direct Numerical Simulations (DNS) is inconclusive at the current time because it does not produce a big enough inertial subrange in order to be able to test pair diffusion laws reliably. For example, Ishihara et al. (2009) perform a DNS with 4096^3 , at Taylor scale based Reynolds numbers $R_\lambda \approx 1200$ showing an approximate inertial subrange energy spectrum over a very short range of just 40. Other DNS of particle pair studies at low Reynolds numbers are, Yeung (1994) at $R_\lambda = 90$, Boffetta & Sokolov (2002) at $R_\lambda = 200$, Ishihara & Kaneda (2002) at $R_\lambda = 283$, Yeung (2004) at $R_\lambda = 230$, Sawford et al. (2008) at $R_\lambda = 650$. Scatamacchia et al. (2012) at $R_\lambda = 300$. See also Bitane et al. (2012), and Biferale et al. (2014). The maximum separation of time scales between the integral time scale and the Kolmogorov times scale observed to date in DNS is about a factor of, 100. This is still about two orders of magnitude smaller than the minimum size required to adequately test inertial subrange pair diffusion scalings. For 2D turbulence, see Jullien et al. (1999), Boffetta & Celani (2000).

Particle Tracking Velocimetry (PTV) laboratory experiments Maas et al. (1993), Malik et al. (1993) have been providing pair diffusion statistics at low to moderate Reynolds numbers. Like DNS, these Reynolds numbers are too small to reliably test pair diffusion laws. Virant & Dracos (1997) obtain pair diffusion measurements from PTV. More recently, Berg et al. (2006) obtained measurements in a water tank at $R_\lambda = 172$, and Bourgoin et al. (2006) and Ouellete et al. (2006) tracked hundreds of particles at high temporal resolution at $R_\lambda = 815$. Although higher resolution tracking experiments using high-energy physics methods have been performed for single particle trajectories La Porta et al. (2001), they have not yet been applied to particle pair studies.

When intermittency is accounted for, the scaling in fully developed turbulence should in fact be slightly greater than the R-O scaling. This will be discussed further in Discussions and Conclusions, Section 6.

Datum Number	Source	Diffusivity K [cm^2/s]	Scale l [cm]
$N1$	Molecular diffusion of oxygen in to ntirogen [1]	1.7×10^{-1}	5×10^{-2}
$N2$	Anemometers 9 m above the ground [2]	3.2×10^3	1.5×10^3
$N3$	Anemometers 21-305 m above the ground [3]	1.2×10^5	1.4×10^4
$N4$	Pilot balloons 100-800 m above the ground [4,5]	6×10^4	5×10^4
$N5$	Tracks of balloons in the atmosphere [6,7]	1×10^8	2×10^6
$N6$	Volcano ash [6,7]	5×10^8	5×10^6
$N7$	Diffusion from cyclones [8]	1×10^{11}	1×10^8

TABLE 1. Datum number, source, the turbulent diffusivity, (K), and the length scale, (l). References: [1] Kay & Laby (1982), [2] Schmidt (1917), [3] Akerblom (1908), [4] Taylor (1915), [5] Hesselberg & Sverdrup (1915), [6] Richardson (1922), [7] Richardson & Proctor (1925), [8] Defant (1921)

3. A reappraisal of the 1926 observational dataset

Richardson (1926) reported in the Proceedings of the Royal Society of London data on turbulent diffusivities collected from different sources, which is reproduced here with a brief description in Table 1. He plotted the turbulent diffusivity against the pair separation in log-log scale, shown as the red and black filled circles in Figure 1. Motivated by an attempt to unify pair diffusional processes across all possible scales, he assumed the scaling $K \sim l^{4/3}$ as a reasonable fit (Fig. 1, dotted blue line). This is not the least squares line of best fit to the data, it is just a theoretical approximation to the data. The actual line of best fit is, $K \sim l^{1.248}$ (Fig. 1, solid red line).

Richardson & Stommel (1948) and Stommel (1949), commenting on diffusion of floats in the sea noted that their new measurements were roughly consistent with the 1926 data, i.e. $K \sim l^{4/3}$. At the end of their paper they wrote, "Note added in proof. After this manuscript was submitted the writers have read two unpublished manuscripts by C. L. von Weisaecker and W. Heisenberg in which the problem of turbulence for large Reynolds number is treated deductively with the result that they arrive at the 4/3 law. The agreement between von Weisaecker and Heisenbergs deduction and our quite independent induction is a confirmation of both", see Benzi (2011). But they also observed that, "any power between $\sim l^{1.3}$ and $\sim l^{1.5}$ would be a tolerable fit to the data". Thus, as early as 1948, it was noted that $K \sim l^{4/3}$ was only a rough fit, which makes it all the more surprising that an alternative theory for pair diffusion has not been developed till now.

However, there is a more fundamental problem with the data. Data-point number $N1$ in Table 1 (Fig. 1, red filled circle) is not from turbulence measurements at all, rather it is from studies of the molecular diffusion of oxygen into nitrogen and whose length scale is stated to be of the order of 10^{-2} cm. At such a small scale it cannot be turbulent, and it cannot contain an extended inertial subrange (even if it were turbulent). This data-point must therefore be disregarded as an outlier in the current investigation which

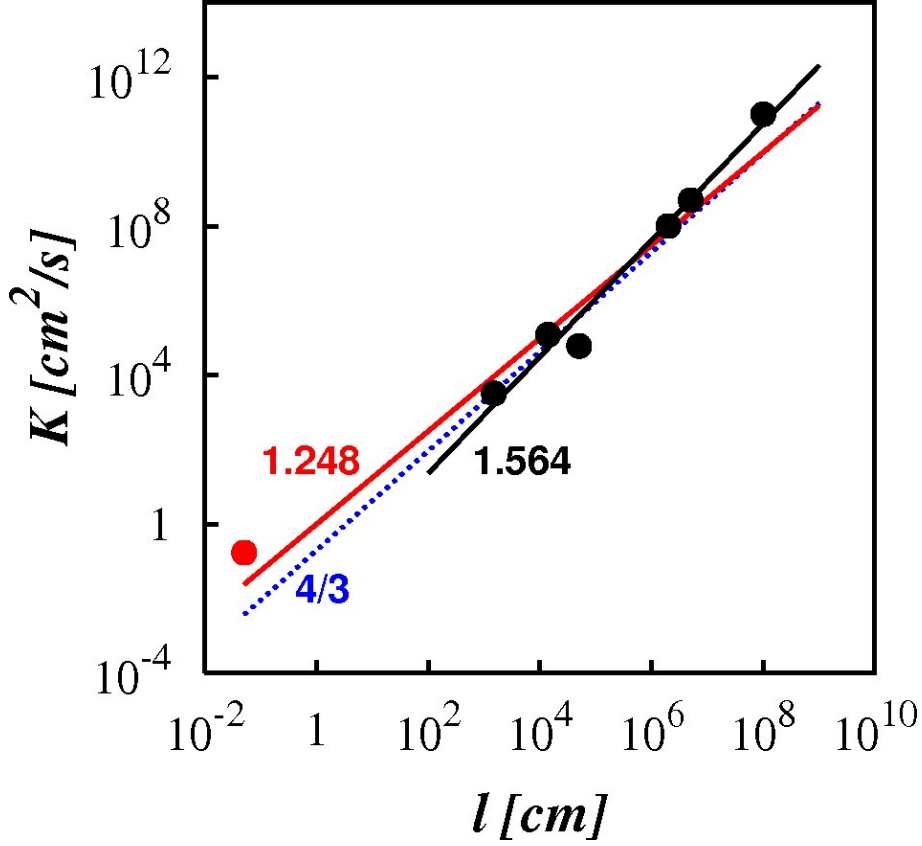


FIGURE 1. The turbulent pair diffusivity against separation, as $\log(K)$ against $\log(l)$. The symbols are the observational data reported by Richardson in 1926 (Table 1). The red filled circle (N1) is from of the molecular diffusion of oxygen into nitrogen. The black filled circles (N2-N7) are from geophysical settings. The dotted blue line is Richardson's assumed locality scaling, $K \sim \sigma_l^{4/3}$. The solid red line is the least square line of best fit to the entire 1926 dataset (N1-N7), $K \sim \sigma_l^{1.248}$. The solid black line is the least square line of best fit to the revised dataset (N2-N7), $K \sim \sigma_l^{1.564}$, and the coefficient of determination is, $R^2 = 0.97$.

strictly demands the existence of turbulence with an extended inertial subrange over several orders of magnitude in scale.

The remaining six data-points (Fig. 1, black filled circles) are sound, coming from geophysical turbulence settings and certainly containing extended inertial subranges. The line of best fit to this new improved dataset (N2 to N7) displays an unequivocal non-local scaling, $K \sim l^{1.564}$ (Fig. 1, solid black line). The coefficient of determination, $R^2 = 0.97$, is very close to 1, meaning that all the data-points lie very close to line of best fit, as is obvious from Figure 1. This implies that the true scaling must be very close this scaling power, probably between $\sim l^{1.5}$ and $\sim l^{1.6}$, which is outside of the bounds noted by Richardson & Stommel, and far from the locality scaling.

The importance of this new finding cannot be under-estimated because it is clear that the 1926 dataset itself implies that turbulent pair diffusional process cannot be purely

local in nature, and therefore non-local diffusional processes cannot be ignored *a priori* in any general theory of pair diffusion, which is where we turn to in the next section.

4. A new theory based upon locality and non-locality

To develop a theory based upon the fundamentally new physical picture that non-local as well as local diffusional processes may play a significant role in the turbulent pair diffusion process, a new mathematical approach is now constructed from which new scaling laws for the turbulent pair diffusivity can be derived. Like Richardson, the focus here is on the diffusivity, which is the most important quantity in the problem; the mean square separation $\langle l^2 \rangle$ is related to the pair diffusivity by the exact relation, $K = 0.5d\langle l^2 \rangle/dt$, and with a general scaling for the diffusivity, $K \sim \sigma_l^\gamma$, there is a the corresponding scaling for $\langle l^2 \rangle \sim t^\chi$. For steady-state equilibrium turbulence χ is given by the exact relation,

$$\chi = \frac{1}{1 - \gamma/2}, \quad 1 < p < 3, \quad (4.1)$$

As such $\langle l^2 \rangle$ does not provide any additional information. We therefore focus our analysis mainly upon K , and refer to $\langle l^2 \rangle$ only where needed in the ensuing analysis and discussions.

To elucidate the role of local and non-local diffusional processes in turbulent pair diffusion, here turbulence with generalized energy spectra, $E(k) \sim k^{-p}$, $k_1 \leq k \leq k_\eta$ with extended inertial subrange, $k_\eta/k_1 \gg 1$, in the power range $1 < p \leq 3$, is considered. The term wavenumber will be used to denote both the vector, \mathbf{k} , as well as its magnitude, $k = |\mathbf{k}|$, and the context will make it clear. Such spectra are routinely used in pair diffusion studies; it helps in understanding the changes in the balance of diffusional processes as the turbulence spectra changes in a way that looking at just Kolmogorov turbulence alone cannot do. In the current work, generalised spectra will play an important mathematical role in validating the new theory for pair diffusion.

The pair diffusivity is now a function of p , i.e. $K(p)$. For some other quantities the subscript p will be used to denote dependence upon the energy spectrum.

4.1. The statement of the problem

The problem is to determine the pair diffusivity, $K = \langle \mathbf{l} \cdot \mathbf{v} \rangle$, of an ensemble of pairs of fluid particles in a field of homogeneous turbulence containing an extended inertial subrange. The particles in a pair are located at $\mathbf{x}_1(t)$ and $\mathbf{x}_2(t)$ at time t , the pair displacement vector is $\mathbf{l}(t) = \mathbf{x}_2(t) - \mathbf{x}_1(t)$, and the pair separation is $l(t) = \sqrt{l_1^2 + l_2^2 + l_3^2} = |\mathbf{x}_2(t) - \mathbf{x}_1(t)|$. The initial separation at some earlier time, t_0 , is denoted by $l_0 = |\mathbf{x}_2(t_0) - \mathbf{x}_1(t_0)|$. The turbulent velocity field is, $\mathbf{u}(\mathbf{x}, t)$, and the particle velocities at time t are, respectively, $\mathbf{u}_1(t) = \mathbf{u}(\mathbf{x}_1(t), t)$ and $\mathbf{u}_2(t) = \mathbf{u}(\mathbf{x}_2(t), t)$, and the pair relative velocity is $\mathbf{v}(l) = \mathbf{u}_2(t) - \mathbf{u}_1(t)$.

As earlier mentioned, Richardson's theory holds strictly in the limit of infinite inertial subrange, implying that $l_0 \rightarrow 0$, as $t \rightarrow 0$. For a large but finite inertial subrange and $l_0 \neq 0$, short time corrections need to be made to the theory, an issue addressed by

Batchelor (1952). It is well known that there exists an initial ballistic regime for very short times due to the high correlation with the initial conditions, which leads to, $\langle l^2 \rangle \sim (t-t_0)^2$ the so-called Batchelor regime. At much larger times, when the pair separation is of the order of the integral length scale, their motions become independent and the pair diffusion collapses to twice the one-particle Taylor diffusion, $\langle l^2 \rangle \rightarrow 2\langle x^2 \rangle \sim t$. These two regimes are well understood and will not be considered any further as the interest here is in the scalings inside the inertial subrange.

In turbulent pair diffusion studies, it is often assumed that the initial pair separation is smaller than the Kolmogorov micro-scale, $l_0 < \eta$, although this is not a formal requirement of the theory. The particles will diffuse apart and eventually decorrelate with the initial conditions, they will 'forget' their initial conditions, (l_0, t_0) , as Batchelor put it, after some travel time, t_{l_0} , when the pair is inside the inertial subrange of turbulent motions. The transition from the Batchelor regime to the explosive inertial subrange regime occurs on a time scale of the order to the eddy turnover time at scale, $\tau_0(l_0)$. If l_0 is already inside the inertial subrange then, $t_{l_0} \approx \tau_0 \sim \varepsilon^{1/3} l_0^{1/3}$.

Without loss of generality, it will be assumed that, $t_0 = 0$. If the pair loses dependency on the initial conditions after some travel time t_{l_0} when the separation, $\delta = \sqrt{\langle l^2 \rangle(t_{l_0})} \ll L$, is well inside the inertial subrange, then it is from $t = t_{l_0}$ that inertial range scaling is assumed to apply. t_{l_0} need not be precisely determined, so long as it is close to when initial conditions have been 'forgotten'. It has been found that taking t_{l_0} to be the time when the pair ensemble distance is equal to the Kolmogorov scale, $\delta = \eta$, gives good numerical results Fung et al. (1992).

When considering generalized power law spectra in simulations, there will be occasions when a start with initial separation greater than the Kolmogorov scale is needed, $\eta < l_0 \ll L$; in these cases, at large times after release but when the pair is still inside the inertial subrange, it is reasonable to approximate with $\delta = l_0$ and $\tau_0 \approx 0$, because $t \gg \tau_0$; the numerical results in Section 6 will justify this approximation. On the basis of the locality hypothesis, the turbulent pair diffusivity is given from dimensional arguments, Richardson (1926), Obukhov (1941), Batchelor (1952), as

$$K \sim \varepsilon^{1/3} \sigma_l^{4/3}, \quad \text{Max}(\eta, \delta) \ll \sigma_l \ll L, \quad t \gg t_{l_0} \quad (4.2)$$

For statistically steady equilibrium turbulence this is equivalent to, $\langle l^2 \rangle \sim t^3$ Obukhov (1941).

4.2. The mathematical framework

The pair relative velocity is, $\mathbf{v} = d\mathbf{l}/dt$, and the pair diffusivity is defined as the ensemble average of the scalar product of \mathbf{v} with \mathbf{l} ,

$$K = \langle \mathbf{l} \cdot \mathbf{v} \rangle \quad (4.3)$$

The interest in this research is in the scaling laws for the pair diffusivity, so a policy of suppressing constants wherever possible will be followed in the rest of the paper.

For homogeneous, isotropic, incompressible, reflectional and statistically stationary turbulence, the Fourier expression for the velocity field \mathbf{u} is, Batchelor (1953),

$$\mathbf{u}(\mathbf{x}) = \int \mathbf{A}(\mathbf{k}) \exp(i\mathbf{k} \cdot \mathbf{x}) d^3\mathbf{k} \quad (4.4)$$

where $\mathbf{A}(\mathbf{k})$ is the Fourier transform of the flow field, \mathbf{k} is the associated wavenumber. The quantity of interest is the relative velocity \mathbf{v} across a finite displacement \mathbf{l} ,

$$\mathbf{v}(\mathbf{l}) = \mathbf{u}(\mathbf{x}_2) - \mathbf{u}(\mathbf{x}_1). \quad (4.5)$$

Using equation (4.4) this gives,

$$\mathbf{v}(\mathbf{l}) = \int \mathbf{A}(\mathbf{k}) [\exp(i\mathbf{k} \cdot \mathbf{l}) - 1] \exp(i\mathbf{k} \cdot \mathbf{x}_1) d^3\mathbf{k}. \quad (4.6)$$

Taking the scalar product of \mathbf{v} with \mathbf{l} and then the ensemble average $\langle \cdot \rangle$ over particle pairs yields an expression for $\langle \mathbf{l} \cdot \mathbf{v} \rangle$; in diffusion studies, it is usual to assume that the Lagrangian ensemble scales with this quantity, see Thomson & Devenish (2005) for example. Thus we obtain a scaling for the pair diffusivity,

$$K \sim \langle \mathbf{l} \cdot \mathbf{v} \rangle \sim \int \langle (\mathbf{l} \cdot \mathbf{A}) [\exp(i\mathbf{k} \cdot \mathbf{l}) - 1] \exp(i\mathbf{k} \cdot \mathbf{x}_1) \rangle d^3\mathbf{k}. \quad (4.7)$$

Because of homogeneity, the ensemble average removes the factor $\exp(i\mathbf{k} \cdot \mathbf{x}_1)$ without altering the scaling upon l . This gives,

$$K(l) \sim \int \langle (\mathbf{l} \cdot \mathbf{A}) [\exp(i\mathbf{k} \cdot \mathbf{l}) - 1] \rangle d^3\mathbf{k}. \quad (4.8)$$

Let k denote the magnitude of the wavenumber, $k = |\mathbf{k}|$. Let $k_l = 1/l$ be the wavenumber associated with the pair separation. As before, the scaling, $l \sim \sigma_l$, will be assumed throughout this work, so that $k_l \sim 1/\sigma_l$, where $\sigma_l^2 = \langle l^2 \rangle$.

It is tempting to approximate the integrand in (4.8) by expanding the exponential term such that, $\exp(i\mathbf{k} \cdot \mathbf{l}) - 1 \approx i\mathbf{k} \cdot \mathbf{l}$. However, such an expansion is accurate only for low wavenumbers $k \ll k_l$ where, $|\mathbf{k} \cdot \mathbf{l}| \ll 1$. For local wavenumbers $k \approx k_l$ where $|\mathbf{k} \cdot \mathbf{l}| \approx 1$, this expansion is approximate and implies some corrections. For high wavenumbers $k \gg k_l$ where $|\mathbf{k} \cdot \mathbf{l}| \gg 1$, this expansion is not accurate.

4.3. Three diffusional processes and uncertainty

A fundamental physical assumption about the nature of the diffusional processes that are occurring in the system is made here, namely it is assumed that there exist three independent diffusional processes that potentially contribute to the pair diffusion process as a whole, each process acting from its own range of wavenumbers relative to the inverse pair separation wavenumber k_l . Partitioning of the spectrum in to different ranges on such a physical basis is often used in turbulence theory, see for example the work on wall turbulence by Perry et al. (2005).

For a given pair separation, σ_l , the three physical processes operate, respectively, from the scales of motion that are smaller than σ_l , from the scales that are local to σ_l , and from the scales that are non-local to σ_l . The associated frequencies are, $\omega(k) \propto \sqrt{k^3 E(k)}$, according to the usual assumption that the frequencies scale with the inverse turnover time of the eddy at wavenumber k . The local eddy frequency is, $\omega_l \propto \sqrt{k_l^3 E(k_l)}$, and the local eddy turnover time is, $T_l \sim 1/\omega_l$.

On this physical basis, the integral in equation (4.8) is partitioned into a sum of three integrals over different wavenumber ranges which are defined by,

s: the small scales such that $k \gg k_l$, and $|\mathbf{k} \cdot \mathbf{l}| \gg 1$, and the associated frequencies are much larger than ω_l , $\omega(k) \gg \omega_l$.

l: the local scales such that $k \approx k_l$, and $|\mathbf{k} \cdot \mathbf{l}| \approx 1$, and the associated frequencies are of the same order as ω_l , $\omega(k) \approx \omega_l$.

nl: the non-local scales such that $k \ll k_l$, and $|\mathbf{k} \cdot \mathbf{l}| \ll 1$, and the associated frequencies are much smaller than ω_l , $\omega(k) \ll \omega_l$.

With this partitioning, (4.8) becomes

$$K \sim \left(\int_{nl} + \int_l + \int_s \right) \langle (\mathbf{l} \cdot \mathbf{A})(\exp(i\mathbf{k} \cdot \mathbf{l}) - 1) \rangle d^3 \mathbf{k}. \quad (4.9)$$

which is rephrased as,

$$K \sim K^{nl} + K^l + K^s \quad (4.10)$$

There is uncertainty in defining the 'size' of a turbulent eddy, a problem which is inherent to the nature of turbulence, Tennekes & Lumley (1972). Consequently, it is not possible to define the precise cut-offs between the local and non-local scales and between the local and small scales of motion.

Although this appears to be an intractable problem, such uncertainty is a defining characteristic of turbulence and is implicit even in the locality hypothesis where a lack of precise definition of the size of a local eddy does not prevent scaling laws from being obtained. Likewise, as the ensuing analysis will show, the general scaling for the relative diffusivity and some asymptotic results can also be obtained in the more general case considered here.

4.4. The physics of the small scales of motion

A simplification can be made with respect to the small scales of motion whose contribution to the diffusion process is,

$$K^s \sim \int_s \langle (\mathbf{l} \cdot \mathbf{A})(\exp(i\mathbf{k} \cdot \mathbf{l}) - 1) \rangle d^3 \mathbf{k} \quad (4.11)$$

There is no need to evaluate this integral directly, because the net ensemble effect can be assessed on physical grounds alone. K^s is the integral over high wavenumbers and

represents the contribution from scales of turbulent motion which are much smaller than the pair separation, i.e., from $k \gg k_l$. The energy contained in these scales is very small if the energy spectrum decreases as k increases, such as an inverse power law of the type $E(k) \sim k^{-p}$, with $p > 1$.

Furthermore, these small scales are associated with unsteadiness of high frequencies, $\omega^s \gg \omega_l$. Statistically, these high frequency motions induce random and rapid changes in the direction and magnitude of the pair displacement vector.

Overall, the changes in the statistics of the pair separation induced by the action of the high frequency, small scale, low energy, random turbulent velocity fluctuations is expected to be extremely small. It is reasonable to assume that the net ensemble effect of the high wavenumbers in the pair diffusion process is correspondingly small, i.e., $K^s \ll \text{Max}(K^l, K^{nl})$. K^s will therefore be neglected henceforth.

4.5. The physics of the local and non-local scales of motion

With the effect of the small scale contributions eliminated, the simplified expression for the pair diffusivity is,

$$K \sim K^{nl} + K^l \quad (4.12)$$

$$\sim \int_{nl} \langle (\mathbf{l} \cdot \mathbf{A})(\exp(i\mathbf{k} \cdot \mathbf{l}) - 1) \rangle d^3\mathbf{k} + \int_l \langle (\mathbf{l} \cdot \mathbf{A})(\exp(i\mathbf{k} \cdot \mathbf{l}) - 1) \rangle d^3\mathbf{k} \quad (4.13)$$

The expansion of the exponential in the integrand to leading order is accurate only in the non-local range where $|\mathbf{k} \cdot \mathbf{l}| \ll 1$. In the local range where $|\mathbf{k} \cdot \mathbf{l}| \approx 1$, such an expansion is only approximately true. Such local eddies are moderately unsteady with frequencies that are of the same order of magnitude as, ω_l . The effect on the local diffusion process is assumed to be likewise moderate, without killing it entirely.

Hence, it is assumed that the ensemble effect of the unsteadiness in the local wavenumbers is to quantitatively reduce the magnitude of the local diffusivity, K^l , but without altering its overall scaling behaviour. Then, the expansion, $\exp(i\mathbf{k} \cdot \mathbf{l}) - 1 \approx i\mathbf{k} \cdot \mathbf{l}$, can be used in (4.13) but with the magnitude of K^l reduced by some factor, $F_l \lesssim 1$, which is smaller than unity, but not too small. Then (4.13) becomes,

$$K \sim \int_{nl} \langle (\mathbf{l} \cdot \mathbf{A})(i\mathbf{k} \cdot \mathbf{l}) \rangle d^3\mathbf{k} + F_l \int_l \langle (\mathbf{l} \cdot \mathbf{A})(i\mathbf{k} \cdot \mathbf{l}) \rangle d^3\mathbf{k} \quad (4.14)$$

$F_l = F_l(p, R_l, C)$ is not expected to be a universal constant because it will depend upon various parameters, like p , and $R_l = k_l/k_1$ which is the size of the inertial subrange relative to the particle pair separation, and also implicitly upon the size of an eddy in wavenumber space, C (to be defined later). After absorbing constants, the integrands in (4.14) become,

$$\langle l^2 |\mathbf{A}| |\mathbf{k}| \cos(\alpha) \cos(\beta) \rangle \quad (4.15)$$

where α is the angle between \mathbf{l} and \mathbf{A} , and β is the angle between \mathbf{l} and \mathbf{k} . For isotropic

random fields averaging (4.15) over all directions, again, does not affect the scaling behaviour. α and β are not uniformly distributed in all direction, it is well known that \mathbf{l} aligns preferentially in the positive strain directions, and this ensures that the ensemble average above is non-zero.

Retaining the angled brackets $\langle \cdot \rangle$ to include averaging over all directions, (4.14) with (4.15) then simplify to,

$$K(l) \sim \int \int_{nl} \langle l^2 ak \rangle dk dA(k) + F_l \int \int_l \langle l^2 ak \rangle dk dA(k) \quad (4.16)$$

where $a = |\mathbf{A}|$, and $dA(k)$ is the element of surface area at radius k in wavenumber space. If the closure, $\langle l^2 ak \rangle \sim \langle l^2 \rangle \langle ak \rangle$, is assumed, then upon integrating over the surface area this integral becomes

$$K(l) \sim \left(\int_{nl} \langle ak \rangle dk + F_l \int_{nl} \langle ak \rangle dk \right) \langle l^2 \rangle. \quad (4.17)$$

Because k and a are magnitudes, then $\langle ak \rangle \neq 0$ even though the vectors \mathbf{k} and \mathbf{A} are orthogonal.

$\int \langle a^2 \rangle dA(k)$ is the energy density per unit wavenumber averaged over all directions, Batchelor (1953), and scales like $\sim E(k)/k$. If the closure, $\int \langle ak \rangle dA(k) \sim k \sqrt{\langle a^2 \rangle dA(k)}$, is assumed then (4.17) becomes,

$$K(l) \sim \left(\int_{nl} \sqrt{kE(k)} dk + F_l \int_{nl} \sqrt{kE(k)} dk \right) \langle l^2 \rangle \quad (4.18)$$

As a further check, this can also be derived as follows. The velocity variance from the scales k to $k+dk$ is $E(k)dk$, and the variance of velocity gradient is $k^2 E(k)dk$. The particle pair velocity variance is, $\sim \langle l^2 \rangle k^2 E(k)dk$. The time scale of eddies of wavenumber k is $1/\sqrt{k^3 E(k)}$. So the incremental contribution to the diffusivity from these scales is the pair velocity variance times the time scale, $dK \sim \langle l^2 \rangle \sqrt{kE(k)} dk$, which leads to (4.18).

To make further progress the actual form of the turbulence spectrum must be specified. In this work, the focus is upon high Reynolds number turbulence which contains an extended inertial subrange. For pair diffusion statistics, the form of the energy spectrum in the large energy containing scales is not important. Such scales do, however, sweep the inertial range eddies which must be modeled. This is implemented by working in the swept frame of reference by setting the spectrum in the large energy scales to zero, $E(k) = 0$ for $k < k_1$, and assuming an inverse power-law energy spectrum in the inertial subrange,

$$E(k) = c \varepsilon^{2/3} L^{5/3-p} k^{-p}, \quad k_1 < k < k_\eta, \quad 1 < p \leq 3 \quad (4.19)$$

where c is a constant. A large length scale L is necessary for dimensional consistency. L scales with some length scale that is characteristic of the large energy scales, such as the integral length scale, or the Taylor length scale.

With the spectrum in (4.19), and with $\sigma_l^2 = \langle l^2 \rangle$, equation (4.18) becomes,

$$K(p) \sim \varepsilon^{1/3} L^{(5/3-p)/2} \left(\int_{nl} k^{(1-p)/2} dk + F_l \int_l k^{(1-p)/2} dk \right) \sigma_l^2 \quad (4.20)$$

This is the most general expression for K that can be derived from the present analysis without any *a priori* assumption regarding locality, other than the partitioning of the spectrum in to local and non-local ranges.

To check the effectiveness of the mathematical approach adopted here in deriving equation (4.20), the locality limit from this expression must first be validated against Richardson's locality hypothesis for which there is a known theory.

4.6. Validation: the locality limit

The assumption of locality means that the non-local (first) term on the right hand side in equation (4.20) is ignored. To evaluate the remaining local integral, some cut-off wavenumber k_* , such that $k_1 < k_* < k_l$, which defines the size of a local eddy in wavenumber space is assumed. Locality is thus assumed valid in the wavenumber range $k_* < k < k_l$, and within this range the wavenumbers k are assumed to scale with k_l . Upon integrating over this range, the local integral in (4.20) yields,

$$K^l(p) \sim \frac{2k_l}{3-p} F_l \varepsilon^{1/3} L^{(5/3-p)/2} \left(1 - \left(\frac{k_*}{k_l} \right)^{(3-p)/2} \right) \sigma_l^2 \quad (4.21)$$

Let the size of an local eddy in wavenumber space be defined by, $C(p, R_l) = k_l/k_*$, where C is finite and greater than unity. $R_l = k_l/k_1$, is related to a local Reynolds number through, $Re_l \sim R_l^{4/3}$. Thus, all dependencies on R_l can be replaced by dependencies on Re_l , e.g. $C = C(p, Re_l)$. We will use R_l in the current analysis. Then (4.21) becomes,

$$K^l(p) \sim \frac{2F_l}{3-p} \varepsilon^{1/3} L^{(5/3-p)/2} k_l^{(3-p)/2} \left(1 - \left(\frac{1}{C} \right)^{(3-p)/2} \right) \sigma_l^2. \quad (4.22)$$

Using the scaling $k_l \sim 1/\sigma_l$, this becomes,

$$K^l(p) \sim F_l \varepsilon^{1/3} L^{(5/3-p)/2} \sigma_l^{\gamma_p^l}, \quad \text{where } \gamma_p^l = (1+p)/2 \quad (4.23)$$

Equation (4.23) reproduces the correct generalized locality scaling, $\gamma_p^l = (1+p)/2$, Morel & Larchaveque (1974), Malik (1996). For Kolmogorov turbulence, $p = 5/3$, this gives, $K_{kol}^l \sim \sigma_l^{4/3}$, which recovers the Richardson's 4/3-scaling law. This validates the mathematical formulation proposed here, justifying the various closures and scaling assumptions that have been made.

4.7. Non-locality: the influence of non-local scales

The important step now is the natural inclusion of the non-local contribution, K^{nl} . As we have observed, *a priori* there is no reason to neglect this term in equation (4.20) – it is locality that has actually emerged in the present approach as an ad hoc assumption.

The non-local contribution is the first term on the right hand side in equation (4.20),

$$K^{nl}(p) \sim \varepsilon^{1/3} L^{(5/3-p)/2} \left(\int_{nl} k^{(1-p)/2} dk \right) \sigma_l^2 \quad (4.24)$$

This is equivalent to strained relative motion; each scale of turbulence that is non-local to the pair separation in the wavenumber range, $k_1 < k < k_*$, will set up a small straining field in the neighbourhood of the pair separation which will alter the rate of increase of the pair separation. Previous theories have always assumed that such non-local effects are negligible. However, there are three factors that suggest that this may be an oversimplification.

Firstly, the non-local wavenumbers, $k_1 < k < k_*$, possess much greater energies than at the local separation wavenumber k_l , and this will increase their relative influence in the pair diffusion process.

Secondly, the time scale of the non-local scales, $T^{nl}(k)$, are much larger than the local turnover time scale, $T^{nl}(k) \gg T_l \sim 1/\omega_l$. This means that the straining fields set up by non-local wavenumber will persist for longer times than the local eddy time scale T_l . This will also enhance their effectiveness in the pair diffusion process.

Thirdly, although an individual non-local wavenumber may indeed have a weak influence, the integral is over a large part of the energy spectrum. Again, this will enhance the effectiveness of the non-local scales in the pair diffusion process.

Taken all together, there is a fair chance that the total non-local contributions are significant. Changing variables in the integrand in equation (4.24) to $s = k/k_1$, yields

$$K^{nl}(p) \sim \varepsilon^{1/3} L^{(5/3-p)/2} k_1^{(3-p)/2} \left(\int_{nl} s^{(1-p)/2} ds \right) \sigma_l^2 \quad (4.25)$$

Inside the integral in equation (4.25) the assumption of non-locality implies that the wavenumbers in range of integration, (k_1, k_*) , do not scale with k_l ; thus the integral inside the brackets is just a definite integral producing a non-dimensional number, $S_{nl} = S_{nl}(p, R_l, C)$; S_{nl} is not expected to be a universal constant. This gives,

$$K^{nl}(p) \sim S_{nl} \varepsilon^{1/3} L^{(5/3-p)/2} k_1^{(3-p)/2} \sigma_l^2 \quad (4.26)$$

If the upper end of the inertial subrange is assumed to scale with the large scale, $k_1 \sim 1/L$, then this simplifies to,

$$K^{nl}(p) \sim S_{nl} \varepsilon^{1/3} L^{-2/3} \sigma_l^{\gamma_p^{nl}}, \quad \text{with } \gamma_p^{nl} = 2, \quad 1 < p \leq 3 \quad (4.27)$$

γ_p^{nl} is the non-locality scaling, and it is equal to 2, independent of p . K^{nl} is thus always strain dominated being proportional to σ_l^2 .

4.8. A general expression for the pair diffusivity

The overall scaling for the turbulent pair diffusivity is the sum of the local and non-local contributions, viz

$$K(p, \sigma_l) \sim O\left(F_l \varepsilon^{1/3} L^{(5/3-p)/2} \sigma_l^{\gamma_p^l}\right) + O\left(S_{nl} \varepsilon^{1/3} L^{-2/3} \sigma_l^2\right), \quad 1 < p \leq 3, \quad (4.28)$$

or simply,

$$K(p) \sim O\left(\sigma_l^{\gamma_p^l}\right) + O\left(\sigma_l^{\gamma_p^{nl}}\right), \quad 1 < p \leq 3, \quad (4.29)$$

where $\gamma_p^l = (1 + p)/2$ is the locality scaling, and $\gamma_p^{nl} = 2$ is the non-locality scaling.

Whereas previous theories for pair diffusion have been based upon simple scaling rules, here a more detailed mathematical approach has been developed by expressing the pair diffusivity through a Fourier integral decomposition. *a priori* assumptions regarding locality have *not* been made, and this has led to an expression for K as the sum of local and non-local contributions in equation (4.29). A feature of this approach is that it uncovers various scalings and closure assumptions that are essential in *any theory* for pair diffusion. Such assumptions are inherent within theories based upon locality scaling rules, but they are often unstated. This is clear from section 4.6 where the correct locality limit was derived using same set of assumptions and closures that has led to the more general expression in equation (4.29).

4.9. The balance of local and non-local processes

The critical question is, what this implies for the overall scaling in K , and how does the diffusivity K actually manifest as a function of σ_l ? It is clear from (4.29) that both local and non-local processes contribute to the pair diffusion process in the range, $1 < p \leq 3$, but there are many uncertainties in their respective magnitudes, and it is not apparent what the relative balance of their contributions is for any given, p , and at any given separation σ_l .

Uncertainty comes from a number of sources, most importantly from the inherent uncertainty in the size of an eddy in wavenumber space, $C(p, R_l)$, of which only a few broad properties can be deduced. It is finite, $1 < C < \infty$, and depends upon p and R_l , and upon the energy spectrum $E(k) \sim k^{-p}$. $\log(E(k))$ becomes shallower as $p \rightarrow 1$, so there is relatively more energy in the local scales as p approaches 1, which indicates that C must increase in this limit, $C \gg 1$. On the other hand, as $p \rightarrow 3$, then $C \rightarrow 1$.

There is also uncertainty in the unknown pre-factors F_l and S_{nl} which account for the various scalings and closures assumed in the analysis.

It would seem impossible to go beyond this point since almost nothing else is known

about the behaviour of C . Fortunately, this problem can be approached from another angle in which neither the exact form of C nor the exact balance of the local and non-local contributions need to be calculated in order to deduce the general scaling for K . It is sufficient to obtain the asymptotic behaviour of C at $p = 1$ and $p = 3$, and the general trend and continuity in the balance as a function of p in the range $1 < p < 3$. These are obtained as follows.

The balance of the local and non-local diffusivities is defined as the ratio, $M_K(p, R_l, C) = K^{nl}/K^l$. M_K is a function of, p, R_l , and C , and it is calculated using equations (4.22), (4.23), (4.25), and (4.26), leading to

$$M_K = \frac{K^{nl}}{K^l} \sim \frac{\left(1 - \left(\frac{C}{R_l}\right)^{(3-p)/2}\right)}{F_l (C^{(3-p)/2} - 1)} \quad (4.30)$$

As, $p \rightarrow 1$, then $M_K \rightarrow (1 - C/R_l)/F_l(C - 1)$. For a large inertial subrange, $R \gg 1$, and with $F_l \approx 0.5$ and $1 \ll C \ll R_l$, then $M_K \rightarrow 1/F_l R_l \ll 1$, and therefore locality dominates in this limit.

As, $p \rightarrow 3$, then $M_K \rightarrow \ln R_l / \ln C - 1$; and with $F_l \approx 0.5$ and, $1 < C \ll R_l^{2/3}$, then $M_K \gg 1$, and therefore non-locality dominates in this limit.

In the intermediate range, $1 < p < 3$, although the balance M_K cannot be obtained quantitatively without the explicit form of F_l and C as a functions of p and R_l , it is instructive to investigate M_K with a wide range of test functions for C to see if any essential trends in the behaviour of M_K can be elucidated. For this purpose, some simplifications are assumed in the following. It is assumed that, $F_l = 0.5$, and for separations deep inside the inertial subrange we set, $R_l = 10^4$. C is then a function of p in these test cases.

The first set of test functions for C are exponential functions, $C(p) = 1.1 + (c_1 - 1.1) \exp(-5(p-1))$, with $C(1) = c_1$, and $C(3) \approx 1.1$. The second set of test functions for C are linear functions, $C(p) = c_1 - (c_1 - 1.1)(p-1)/2$, with $C(1) = c_1$, and $C(3) = 1.1$. A third set of test functions for C are constants, $C(p) = c_1$. In each of these three sets of test cases, M_K was calculated using (4.30) for five selected values of $c_1 = 4, 10, 20, 50$, and 100.

For all the test functions considered, $M_K \gg 1$ as $p \rightarrow 3$, (Figs. 2, 3 and 4), indicating that non-locality is always dominant in this limit. Furthermore, $M_K \ll 1$ as $p \rightarrow 1$, in all the test cases considered, indicating that locality is always dominant in this limit.

Importantly, $M_K(p)$ increases smoothly and monotonically as p increases from 1 to 3 in all the test cases considered. The linear and constant test functions display very similar trends (Figs. 3 and 4), while the exponential test functions (Fig. 2), differ from these by up to a factor of about 10 at any value of p .

Thus, the asymptotic limits of M_K at $p = 1$ and $p = 3$ are observed to be only weakly dependent upon the form of C , and M_K is observed to be a smooth function of p in the range $1 < p < 3$. The following conclusions may therefore be drawn for large inertial subranges where $R_l \gg 1$. Firstly, as $p \rightarrow 1$ then $M_K \ll 1$, and therefore $K^{nl} \ll K^l$, yielding the locality limit,

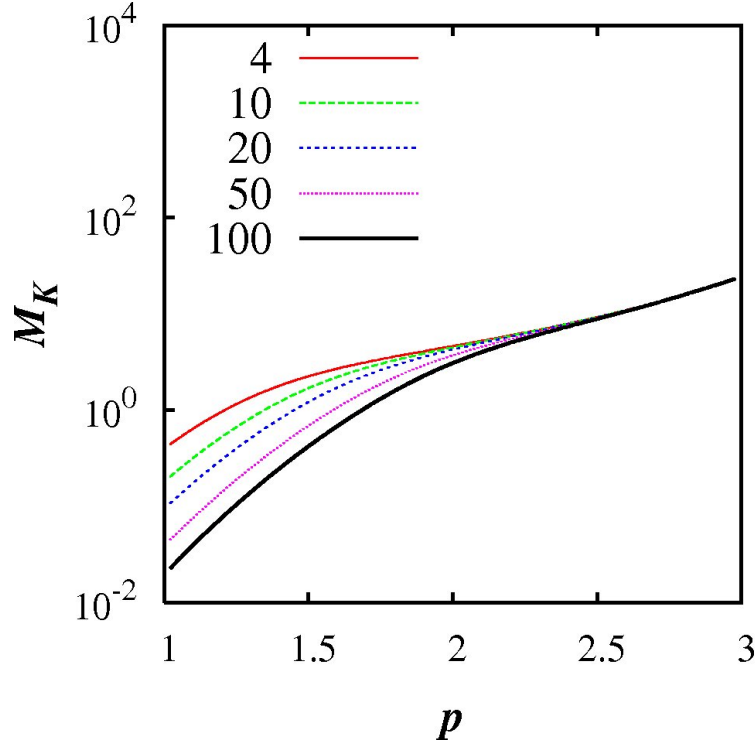


FIGURE 2. The balance $M_K = K^{nl}/K^l$ shown as $\log(M_K)$ against p . Exponential test functions, $C(p) = 1.1 + (c_1 - 1.1) \exp(-5(p - 1))$, were used in M_K in equation (4.30) with $R_l = 10^4$, and $F_l = 0.5$. Five cases are shown, $c_1 = 4, 10, 20, 50, 100$.

$$K(p) \rightarrow K^l(1) \sim \sigma_l^1 \quad \text{as } p \rightarrow 1. \quad (4.31)$$

Secondly, as $p \rightarrow 3$ then $M_K \gg 1$, and therefore $K^{nl} \gg K^l$, yielding the non-locality limit,

$$K(p) \rightarrow K^{nl}(3) \sim \sigma_l^2 \quad \text{as } p \rightarrow 3. \quad (4.32)$$

Thirdly, $M_K(p)$ must also be a smooth function of p in the range $1 < p \leq 3$ and it increases smoothly and monotonically as p increases smoothly from 1 to 3; the non-local scales exert increasingly stronger influence at the local pair separation scale until they are completely dominant.

4.10. The general scaling for K

Since $M_K(p)$ is a smooth and continuous function of p in the range $1 < p \leq 3$, then $K(p)$ must also be a smooth and continuous function of p in this range and it must display a smooth transition between its asymptotic limits, $K(1) \sim \sigma_l^1$ and $K(3) \sim \sigma_l^2$, as p passes smoothly from 1 to 3.

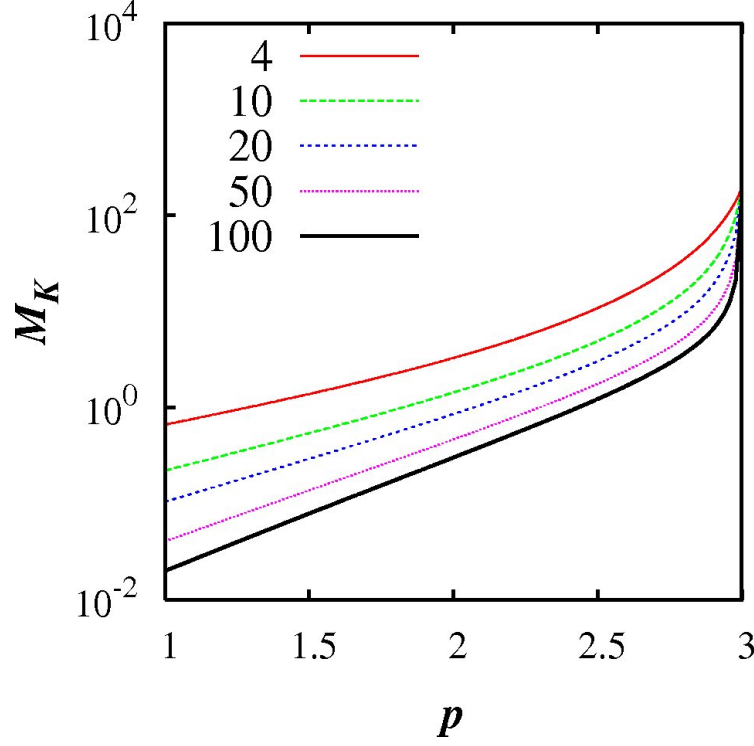


FIGURE 3. The balance $M_K = K^{nl}/K^l$ shown as $\log(M_K)$ against p . Linear test functions, $C(p) = c_1 - (c_1 - 1.1)(p - 1)/2$, were used in M_K in equation (4.30) with $R_l = 10^4$, and $F_l = 0.5$. Five cases are shown, $c_1 = 4, 10, 20, 50, 100$.

It is possible that either one of the local or non-local processes dominates throughout the inertial subrange for any given p ; but that would imply a discontinuous jump between locality and non-locality scalings at some value of p in order to satisfy the asymptotic limiting cases in (4.31) and (4.32). This is unlikely, and also violates the continuity in $K(p)$ as a function of p .

It is also possible that for every p both local and non-local power laws exist in different parts of the inertial subrange, with a crossover between them in the middle of the inertial subrange. In this case some new, as yet unknown, crossover separation scale $l_c(p)$ has to be introduced in to the theory. This is also unlikely, and no evidence for such a cross-over length scale exists.

A third possibility is that both local and non-local diffusional processes are effective in the pair diffusion process inside the inertial subrange for all p in the range, $1 < p \leq 3$, at all separations where the new theory is valid. Then, for any given turbulence spectrum, $E(k) \sim k^{-p}$, the pair diffusivity $K(p)$ must manifest as a smooth transition between the two asymptotic limits, (4.31) and (4.32), over the range of separations for which it is valid. Since $K(p)$ also satisfies (4.29) then it must be a power law scaling which is intermediate between the purely local and non-local scalings,

$$K(p) \sim \sigma_l^{\gamma_p}, \quad \text{with } \gamma_p^l < \gamma_p < \gamma_p^{nl}, \quad \text{for } 1 < p < 3. \quad (4.33)$$

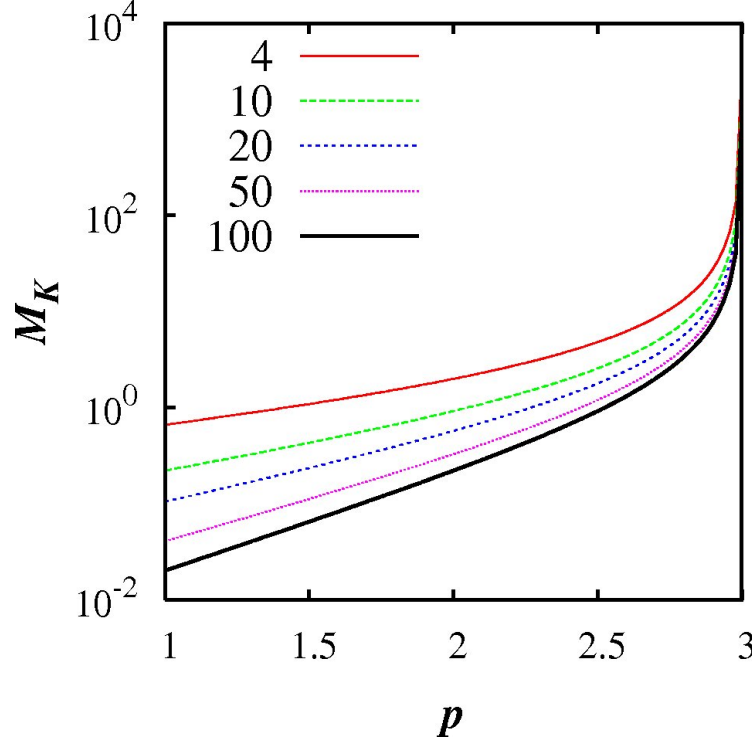


FIGURE 4. The balance $M_K = K^{nl}/K^l$ shown as $\log(M_K)$ against p . Constant test functions, $C(p) = c_1$, were used in M_K in equation (4.30) with $R_l = 10^4$, and $F_l = 0.5$. Five cases are shown, $c_1 = 4, 10, 20, 50, 100$.

The new scaling powers γ_p are such that, as $p \rightarrow 1$ then $\gamma_p \rightarrow 1$, and as $p \rightarrow 3$ then $\gamma_p \rightarrow 2$. Globally, $1 < \gamma_p \leq 2$. Furthermore, γ_p must transform smoothly between these limiting cases as p goes from 1 to 3. Note that $\gamma_p = 2$ is attained only when, $p = 3$.

Equation (4.33) is the main prediction of the new theory, with $\gamma_p^l = (1 + p)/2$ and $\gamma_p^{nl} = 2$. It is equivalent to the mean square separation scaling, $\langle l^2 \rangle \sim t^{\chi_p}$, with χ_p given by $\chi_p = 1/(1 - \gamma_p/2)$ from equation (4.1).

For Kolmogorov turbulence, $E \sim k^{-5/3}$, the new theory predicts that, $\gamma_{Kol} > 4/3$. For real turbulence which includes intermittency $\mu_I > 0$, such that $E \sim k^{-(5/3+\mu_I)}$, the scaling should be higher with $\gamma_{\mu_I} > \gamma_{\mu_I}^l = 4/3 + \mu_I/2$.

The new theory implies that a non-Richardson 4/3-law, $K \sim \sigma_l^{4/3}$, exists for some spectrum, $E \sim k^{-p_*}$, with $p_* < 5/3$ where $\gamma_{p_*} = 4/3$. This is equivalent to $\langle l^2 \rangle \sim t^3$, which is a new t^3 -regime for the mean square separation.

The ratio of the non-local and local power scaling is defined as,

$$M_\gamma(p) = \frac{\gamma_p}{\gamma_p^l} \quad (4.34)$$

$M_\gamma(p)$ is equal to 1 at both $p = 1$ and $p = 3$, and since $M_\gamma > 1$ in the range $1 < p < 3$,

then there must be a maximum in M_γ at some $p = p_m$ for an energy spectrum $E \sim k^{-p_m}$, where $1 < p_m < 3$.

The new theory predicts only the upper and lower bounds for the scaling powers, equation (4.33), but it holds for a wide range of power spectra, $1 < p \leq 3$. The available data exists only for a single spectrum, although a very important one, for real turbulence including intermittency for which the geophysical data, Fig. 1, suggests a scaling of, $\gamma_{\mu_I} \approx 1.564$, i.e. $K_{\mu_I}(p) \sim \sigma_l^{1.564}$.

5. Numerical calculations using a Lagrangian diffusion model

We have developed a new non-local theory for turbulent particle pair diffusion, and seen that it predicts scaling laws for the pair diffusivity, K , equation (4.33), which is consistent with the reappraised 1926 data from geophysical turbulence, Fig. 1.

However, the values of γ_p cannot be predicted from the theory alone. To do this, and to examine other predictions of the new theory, ideally we need experiments and/or DNS. Unfortunately, current capabilities of both experiments and DNS are far from being able to examine very large inertial subrange turbulence, as seen in Sections 2 and 3. However, we can make some progress in examining the theory through the use of Lagrangian diffusion models.

Lagrangian diffusion models, like random walk models, do not necessarily satisfy Navier-Stokes equations, but they can be indicative of the scaling behaviour of Lagrangian statistics in fluid flows, sometimes quite accurately. Furthermore, neither is Richardson's theory based upon satisfying Navier-Stokes equation, so in the present study Lagrangian diffusion models may be able to shed some useful light on to this problem.

5.1. Particle trajectories using KS

In this study, the Lagrangian diffusion model Kinematic Simulations (KS) was used to obtain the statistics of particle pair diffusion. In KS one specifies the second order Eulerian structure function through the power spectrum, Kraichnan (1970), Fung et al. (1992). KS is particularly useful here because it can generate extended inertial subranges sufficient to test inertial subrange pair diffusion scaling laws. Pair diffusion statistics were thus obtained from KS containing generalized energy spectra, $E(k) \sim k^{-p}$, $k_1 \leq k \leq k_\eta$ over extended inertial subranges with $k_\eta/k_1 = 10^6$, and for $1 < p \leq 3$.

KS generates turbulent-like non-Markovian particle trajectories by releasing particles in flow fields which are prescribed as sums of energy-weighted random Fourier modes. By construction, the velocity fields are incompressible and the energy is distributed among the different modes by a prescribed Eulerian energy spectrum, $E(k)$. The essential idea behind KS is that the flow structures in it - eddying, straining, and streaming zones - are similar to those observed in turbulent flows, although not precisely the same. This is sufficient to generate turbulent-like particle trajectories.

KS has been used to examine single particle diffusion Turfus & Hunt (1987), and pair diffusion Fung et al. (1992), Malik (1996), Fung & Vassilicos (1998), Malik & Vassilicos (1999), Nicolleau & Nowakowski (2011). KS has also been used in studies of turbulent diffusion of inertial particles Maxey (1987), Meneguz & Reeks (2011), Farhan et al.

(2015). Meneguz & Reeks found that the statistics of the inertial particle segregation in KS generated flow fields for statistically homogeneous isotropic flow fields are similar to those generated by DNS. KS has also been used as a sub-grid scale model for small scale turbulence Perkins et al. (1993), Yao & He (2009).

5.2. The KS velocity fields and energy spectra

An individual Eulerian turbulent flow field realization is generated as a truncated Fourier series,

$$\mathbf{u}(\mathbf{x}, t) = \sum_{n=1}^{N_k} \left((\mathbf{A}_n \times \hat{\mathbf{k}}_n) \cos(\mathbf{k}_n \cdot \mathbf{x} + \omega_n t) + (\mathbf{B}_n \times \hat{\mathbf{k}}_n) \sin(\mathbf{k}_n \cdot \mathbf{x} + \omega_n t) \right) \quad (5.1)$$

where N_k is the number of representative wavenumbers, typically hundreds for very long spectral ranges, $k_\eta/k_1 \gg 1$. $\hat{\mathbf{k}}_n$ is a random unit vector; $\mathbf{k}_n = k_n \hat{\mathbf{k}}_n$ and $k_n = |\mathbf{k}_n|$. The coefficients \mathbf{A}_n and \mathbf{B}_n are chosen such that their orientations are randomly distributed in space and uncorrelated with any other Fourier coefficient or wavenumber, and their amplitudes are determined by $\langle \mathbf{A}_n^2 \rangle = \langle \mathbf{B}_n^2 \rangle \propto E(k_n) dk_n$, where $E(k)$ is the energy spectrum in some wavenumber range $k_1 \leq k \leq k_\eta$. The angled brackets $\langle \cdot \rangle$ denotes the ensemble average over particles and over many random flow fields. The associated frequencies are proportional to the eddy-turnover frequencies, $\omega_n = \lambda \sqrt{k_n^3 E(k_n)}$. There is some freedom in the choice of λ , so long as $0 \leq \lambda < 1$. The construction in equation (5.1) ensures that the Fourier coefficients are normal to their wavevector which automatically ensures incompressibility of each flow realization, $\nabla \cdot \mathbf{u} = 0$. The flow field ensemble generated in this manner is statistically homogeneous, isotropic, and stationary.

Unlike some other Lagrangian methods, by generating entire kinematic flow fields in which particles are tracked KS does not suffer from the crossing-trajectories error which is caused when two fluid particles occupy the same location at the same time in violation of incompressibility; but because KS flow fields are incompressible by construction this error is completely eliminated.

Intermittency exists in KS because flow structures such as vortex tubes exist in the flow field, although they are not exactly the same as in fully dynamic turbulence, Fung et al. (1992). By adjusting the power spectrum we can mimic the intermittent spectrum seen in real turbulence. KS pair diffusion statistics have been validated and found to produce close agreement with DNS, at least for low Reynolds numbers, Malik & Vassilicos (1999), including the flatness factor of pair separation.

The energy spectrum $E(k)$ can be chosen freely within a finite range of scales, even a piecewise continuous spectrum, or an isolated single mode are possible. To incorporate the effect of large scale sweeping of the inertial scales by the energy containing scales, the simulations are carried out in the sweeping frame of reference by setting $E(k) = 0$ in the largest scales, for $k < k_1$, and an inverse power spectrum in the inertial subrange,

$$E(k) = C_k^{2/3} L^{5/3-p} k^{-p}, \quad k_1 \leq k \leq k_\eta, \quad 1 < p \leq 3 \quad (5.2)$$

where C_k is a constant. The largest represented scale of turbulence is $2\pi/k_1$ and smallest

is the Kolmogorov micro-scale $\eta = 2\pi/k_\eta$. L is some large length scale, such as the integral length scale, or a Taylor length scale.

A particle trajectory, $\mathbf{x}_L(t)$, is obtained by integrating the Lagrangian velocity, $\mathbf{u}_L(t)$, in time,

$$\frac{d\mathbf{x}_L}{dt} = \mathbf{u}_L(t) = \mathbf{u}(\mathbf{x}, t). \quad (5.3)$$

Pairs of trajectories are harvested from a large ensemble of flow realizations and pair statistics are then obtained from it for analysis.

5.3. KS Parameters

The spectrum in (5.2) is normalized such that the total energy density contained in any flow realization is $3u'/2$, where u' is the rms turbulent velocity fluctuations in each direction.

In the current simulations, $k_1 = 1, L = 1, C_k = 1.5$ (Kolmogorov constant) and $u' = 1$. Then this yields,

$$\varepsilon^{2/3} = (p-1) \left(1 - \left(\frac{k_1}{k_\eta} \right)^{p-1} \right)^{-1} \quad (5.4)$$

$p = 1$ is a singular limit which is not consider here. The size of the inertial subrange is fixed in all the simulations here at, $k_\eta/k_1 = 10^6$. With (5.4), $v_\eta = (\varepsilon\eta)^{1/3}$ is the velocity micro-scale, and $t_\eta = \varepsilon^{-1/3}\eta^{2/3}$ is the time micro-scale.

The distribution of the wavenumbers is geometric, $k_n = r^{n-1}k_1$, and the common ratio is $r = (k_\eta/k_1)^{1/(N_k-1)}$. The increment in wavenumber-space of the n th wavenumber is $\Delta k_n = k_n(\sqrt{r} - 1/\sqrt{r})$. The frequency factor is chosen to be, $\lambda = 0.5$, which is typical in many KS studies. A choice of $\lambda < 1$ does not affect the scaling in the pair diffusivity, even frozen turbulence, $\lambda = 0$, has been found to yield the same scaling, which has been attributed to the open streamline topology of streamlines in 3D flows, Malik (1996).

It is important to simulate cases over the whole range of in the energy spectrum $1 < p \leq 3$, in order to examine the new theory comprehensively.

5.4. Simulation Results

The spectra in equation (5.2) were prescribed in the KS simulations. 25 cases of p were selected in the range, $1 < p \leq 3$. The case $p = 1$ is singular, but p can be taken close to this limit; the smallest value of p chosen was, 1.01 (Table 2).

The particle trajectories were obtained by integrating (5.3) using the 4th order Adams-Bashforth predictor-corrector method (4th order Runge-Kutta gives identical results). Thomson & Devenish (2005) used a variable time step t that was small compared to the turnover time of an eddy of the size of the instantaneous pair separation, but larger than

p	γ_p	γ_p^l	χ_p	χ_p^l	M_γ
1.01	1.060	1.005	2.128	2.010	1.055
1.1	1.120	1.05	2.273	2.105	1.067
1.2	1.190	1.10	2.469	2.222	1.082
1.3	1.260	1.15	2.703	2.353	1.096
1.4	1.340	1.20	3.030	2.500	1.117
1.5	1.410	1.25	3.390	2.667	1.128
1.6	1.480	1.30	3.846	2.857	1.139
5/3	1.525	4/3	4.211	3	1.144
1.70	1.545	1.35	4.396	3.077	1.144
1.72	1.555	1.360	4.494	3.125	1.143
1.74	1.570	1.370	4.651	3.175	1.146
1.77	1.585	1.385	4.819	3.252	1.144
1.8	1.605	1.40	5.063	3.333	1.146
1.9	1.660	1.45	5.882	3.636	1.145
2.0	1.710	1.50	6.897	4	1.140
2.1	1.750	1.55	8.000	4.444	1.129
2.2	1.790	1.60	9.424	5	1.119
2.3	1.820	1.65	11.11	5.714	1.103
2.4	1.850	1.70	13.33	6.676	1.088
2.5	1.880	1.75	16.67	8	1.074
2.6	1.900	1.80	20.00	10	1.056
2.7	1.930	1.85	28.57	13.33	1.043
2.8	1.950	1.90	40.00	20	1.026
2.9	1.970	1.95	67.67	40	1.010
3.0	2.000	2.00	∞	∞	1.000

TABLE 2. $p, \gamma_p, \gamma_p^l, \chi_p, \chi_p^l$, and M_γ . The pair diffusivity is, $K \sim \sigma_l^{\gamma_p}$, the locality scaling is, $\gamma_p^l = (1 + p)/2$. The mean square separation is, $\langle l^2 \rangle = t^{\chi_p}$, where $\chi_p = 1/(1 - \gamma_p/2)$, and the locality scaling is, $\chi_p^l = 1/(1 - \gamma_p^l/2)$. The ratio of the power scalings is, $M_\gamma = \gamma_p/\gamma_p^l$.

the turbulence micro-scale t_η . While this speeds up the turnaround time of the calculations, here it is desired to avoid extra assumptions so that unambiguous conclusions can be drawn from the results. Therefore, in all of the current simulations a very small but fixed time step, $\Delta t \ll t_\eta$ has been used. This has the further advantage of avoiding any smoothening of the particle trajectories that is necessary when using variable time steps.

Eight pairs of a particles were released in each flow realization, placed initially at the corners of a cube of side 3 units, beginning at $(0, 0, 0)$. This is far enough apart for each pair to be independent. It is crucial to run over a large number of different flow realizations, otherwise the statistics will not converge. Typically the ensemble was around 5000 flow realizations, yielding a harvest of 40,000 particle pair trajectories per simulation. A simulation was run for about one large timescale, $T = 2\pi/k_1$, which required around 10^6 time steps.

The results obtained from KS are summarized in Table 2. This table shows γ_p from

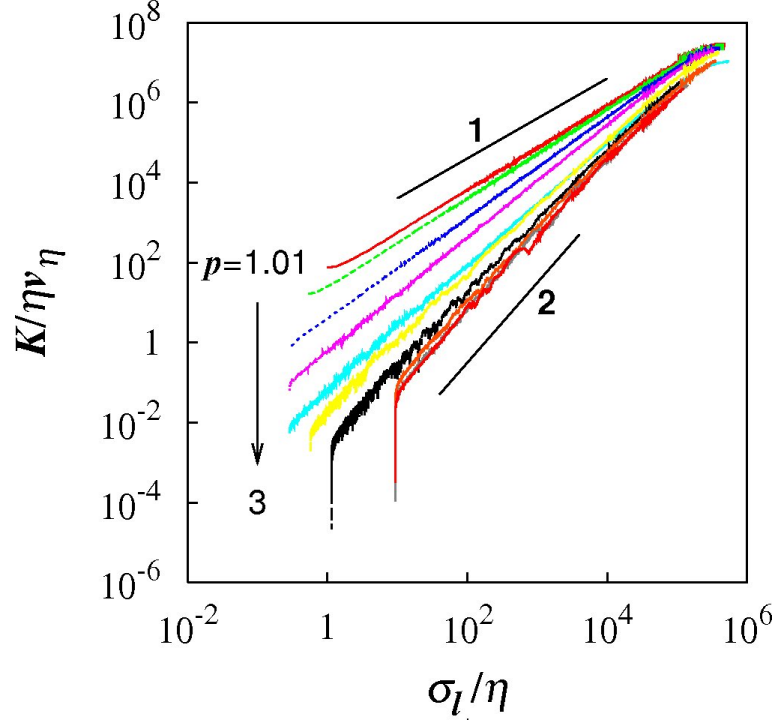


FIGURE 5. The turbulent pair diffusivity as $\log(K/\eta v_\eta)$ against $\log(\sigma_l/\eta)$. The results were obtained from Kinematic Simulations. The KS energy spectra used were, $E(k) \sim k^{-p}$, with the inertial subrange, $k_\eta/k_1 = 10^6$. 25 cases cover the range $1 < p \leq 3$, (Table 2); but for clarity only 10 cases are shown here: $p = 1.01, 1.1, 1.3, 1.5, 5/3, 1.9, 2.2, 2.5, 2.9, 3.0$. The slopes, γ_p , show a smooth transition from $p = 1.01$ to 3. Solid black lines of slopes 1 and 2 are shown for comparison.

the simulations in column 2; $\gamma_p^l = (1 + p)/2$ in column 3. The equivalent mean square separation scaling laws, $\langle l^2 \rangle \sim t^\chi$, are also shown: $\chi_p = 1/(1 - \gamma_p/2)$ is the non-local scaling, column 4; $\chi_p^l = 1/(1 - \gamma_p^l/2) = 4/(3 - p)$ is the local scaling, column 5. The ratio of scaling powers, $M_\gamma(p) = \gamma_p/\gamma_p^l$ is shown in column 6.

Log-log plots of the turbulent pair diffusivity $K/\eta v_\eta$ against the separation σ_l/η for different energy spectra p display clear power law scalings of the form,

$$K(p) \sim \sigma^{\gamma_p}, \quad 1 < \gamma_p \leq 2, \quad 1 < p \leq 3, \quad (5.5)$$

over wide ranges of the separation inside the inertial subrange (Fig. 5). The γ_p 's are the slopes of the plots in Figure 5; these are more easily observed by plotting the compensated relative diffusivity $K/\sigma_l^{\gamma_p}$ against the separation (Fig. 6). The γ_p 's are the powers that give near-horizontal lines over the longest range of separation, a procedure that determines γ_p to within 1% error for most p , except near the singular limit, $p = 1$, where the errors are around 6%.

The plots of γ_p and $\gamma_p^l = (1 + p)/2$ against p show that the new scaling powers, γ_p , are in the range, $(1 + p)/2 < \gamma_p \leq 2$, (Fig. 7, black filled circles and dotted blue line

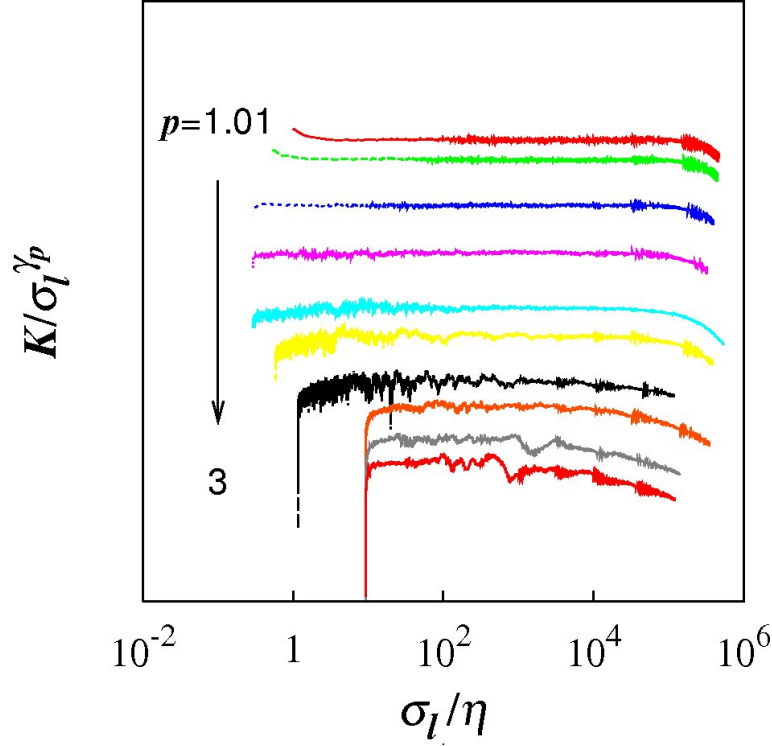


FIGURE 6. Compensated turbulent pair diffusivity as $\log(K/\sigma_l^{\gamma_p})$ against $\log(\sigma_l/\eta)$. The colour coding is similar to that in Figure 5. The values of, γ_p , (Table 2) are the ones that display the best near horizontal line over the longest separation range. For clarity some of the plots have been spaced out vertically, hence no scale is shown on the ordinate. This does not affect the scaling which is the main interest here.

respectively, left hand scale). It is observed that as $p \rightarrow 1$, then $\gamma_p \rightarrow 1$; and as $p \rightarrow 3$, then $\gamma_p \rightarrow 2$. Furthermore, the, γ_p 's, display a smooth transition between the asymptotic limits at $p = 1$ and 3.

The range of separation over which the scalings, $K(p) \sim \sigma_l^{\gamma_p}$, are observed to progressively reduce from both ends of the range as $p \rightarrow 3$. It reduces from below due to the diminishing energies contained in the smallest scales so that the pair separation penetrates further into the inertial subrange before it 'forgets' the initial separation. It reduces from above because the long range correlations are increasingly stronger as $p \rightarrow 3$ causing the particles in a pair to become independent at earlier times and at smaller separation.

The plot of M_γ against p show a peak at $p_m \approx 1.8$, where $M_\gamma(p_m) \approx 1.15$, (Fig. 7, right hand scale). In fact, M_γ remains relatively close to this peak value in a neighbourhood of $p = 1.8$, in the range $1.5 < p < 2$.

Plots of the scaling powers, χ_p , obtained from the simulations (filled black circles), and from $\chi_p^l = 4/(3-p)$ (dotted blue line), against p are shown in Figure 8. The same is shown in Figure 9, but focussing in the range $1.5 < p < 2$ which covers the intermittent turbulence range which is indicated by the two red vertical lines.

For Kolmogorov turbulence, $p = 5/3$, KS produces, $\gamma_{Kol} \approx 1.525$, so that $K_{Kol} \sim \sigma_l^{1.525}$.

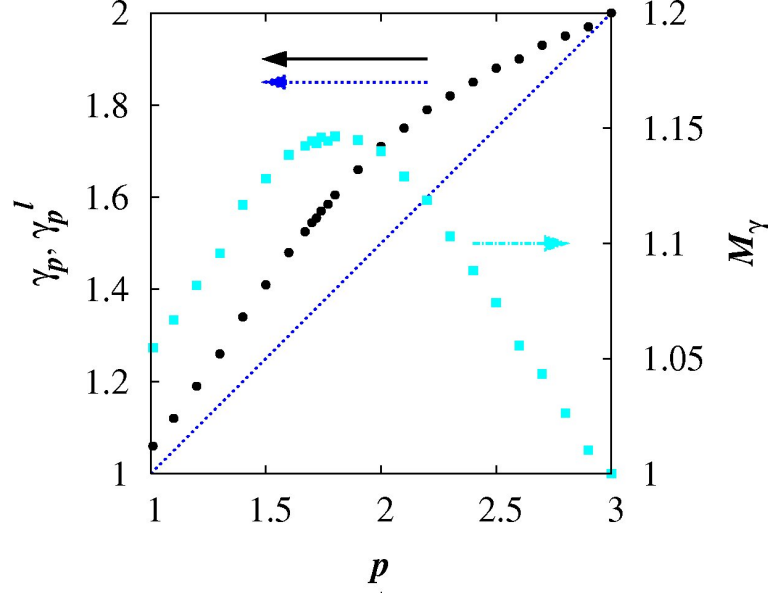


FIGURE 7. γ_p , γ_p^l , and M_γ against p . The black filled circles are the γ_p 's. The dotted blue line is the locality scaling $\gamma_p^l = (1+p)/2$. The cyan squares are the ratios, $M_\gamma = \gamma_p/\gamma_p^l$ (right hand scale), (Table 2).

For real turbulence with intermittency corrections, $\mu_I > 0$, such that $E(k) \sim k^{-(5/3+\mu_I)}$, three extra cases, $p_I = 5/3 + \mu_I$, where simulated. The currently accepted value for the intermittency lies in the range, $0.025 < \mu_I < 0.075$, Anselmet et al. (2001), Tsuji (2004), Meyers & Meneveau (2008), Tsuji (2009). Therefore, three cases that cover most of this range were simulated, $p_I = 1.70, 1.72$, and 1.74 . For these spectra, KS produced, (Fig. 7 and Table 2),

$$\begin{aligned} K_{\mu_I} &\sim \sigma_l^{1.545}, & \text{for } p_I = 1.70, \quad \mu_I = 0.033 \\ K_{\mu_I} &\sim \sigma_l^{1.555}, & \text{for } p_I = 1.72, \quad \mu_I = 0.053 \\ K_{\mu_I} &\sim \sigma_l^{1.570}, & \text{for } p_I = 1.74, \quad \mu_I = 0.073 \end{aligned} \quad (5.6)$$

The mid-point in the above intermittency range is close to, $p_I = 1.72$, which gives the scaling law $K_{\mu_I} \sim \sigma_l^{1.555}$, which is an error of less than 0.6% in the scaling power compared to the data in Figure 1. For, $p_I = 1.70$, we obtain $K_{\mu_I} \sim \sigma_l^{1.545}$, and the error in the scaling power is 1.2%; for $p_I = 1.74$, we obtain $K_{\mu_I} \sim \sigma_l^{1.570}$, and the error in the scaling power is 0.4%. It is reasonable to infer that the error will be almost zero close to $p_I \approx 1.73$.

The Kolmogorov spectrum $p = 5/3$ produces, $K_{Kol} \sim \sigma_l^{1.525}$, and the error in the scaling power is 2.5%. The Richardson's locality law, $K \sim \sigma_l^{4/3}$, is 15% in error in the scaling power compared to the reappraised geophysical data in Figure 1.

The simulations produce scalings for $\langle l^2 \rangle \sim t^{x_p}$, in the range $\sim t^{4.494}$ to $\sim t^{4.615}$ for the same intermittent spectra considered above, Fig. 9, Table 2. It is interesting to note that

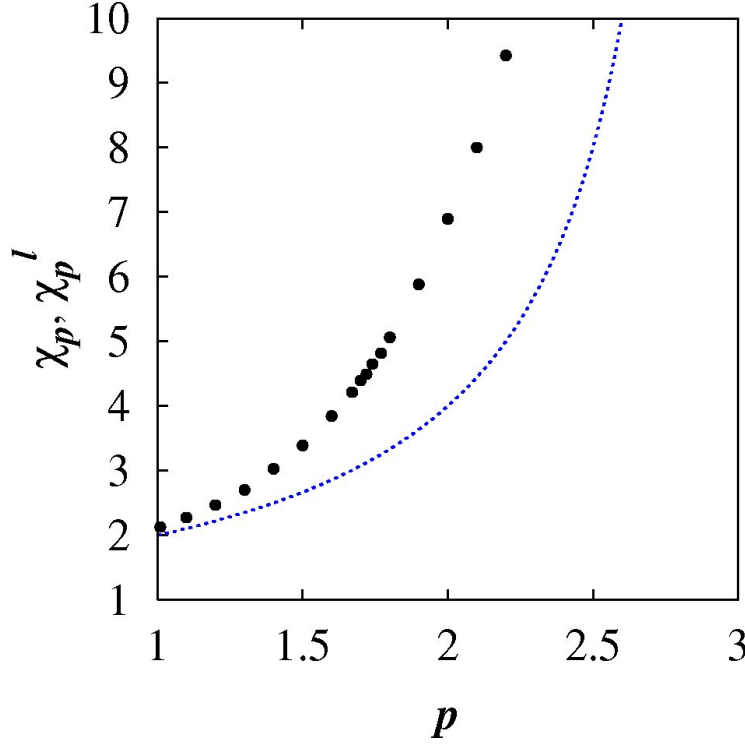


FIGURE 8. χ_p, χ_p^l , against p . The black filled circles are, χ_p 's from the simulations. The dotted blue line is the locality scaling, $\chi_p^l = 4/(3-p)$. See Table 2.

even under the assumption of locality intermittency spectra should produce scalings in the range $\langle l^2 \rangle \sim t^{3.077}$ to $\sim t^{3.252}$ – thus, a true R-O t^3 -regime cannot exist in reality.

In general KS predicts the correct scaling for the turbulent pair diffusivity to within 1% of the geophysical data in Figure 1 in most of the accepted intermittency range centred in the neighbourhood of, $E(k) \sim k^{-1.73}$.

Finally, KS produces a non-Richardson 4/3-scaling, $K \sim \sigma_l^{4/3}$, where $\gamma_{p_*} = 4/3$ at $p_* \approx 1.4$, (Fig. 7 and Table 1). With this spectrum, $E(k) \sim k^{-1.4}$, this is equivalent to a new $\langle l^2 \rangle \sim t^3$ regime.

5.5. Estimate of numerical errors

The numerical results presented here are the most comprehensive obtained to date from KS due to the very large ensemble of particle pairs and the small time steps used. The statistical fluctuations in the results are therefore small. The γ_p 's, which are the slopes of the plots in Figure 5, can be determined to within 1% error. An exception is close to the singular limit $p = 1$ where the numerical errors can be large. An accurate estimate of this error can be obtained as follows, noting first that the error level in γ_p is identical to the error level in M_γ . As $p \rightarrow 1$, then $M_\gamma \rightarrow 1$; but very close to this limit, $M_\gamma \approx 1$ is still a good approximation. For $p = 1.01$, KS produces, $M_\gamma \approx 1.06$ (Fig. 7 and Table 1). This is an error of 6% which is small considering that it is so close to the singular limit.

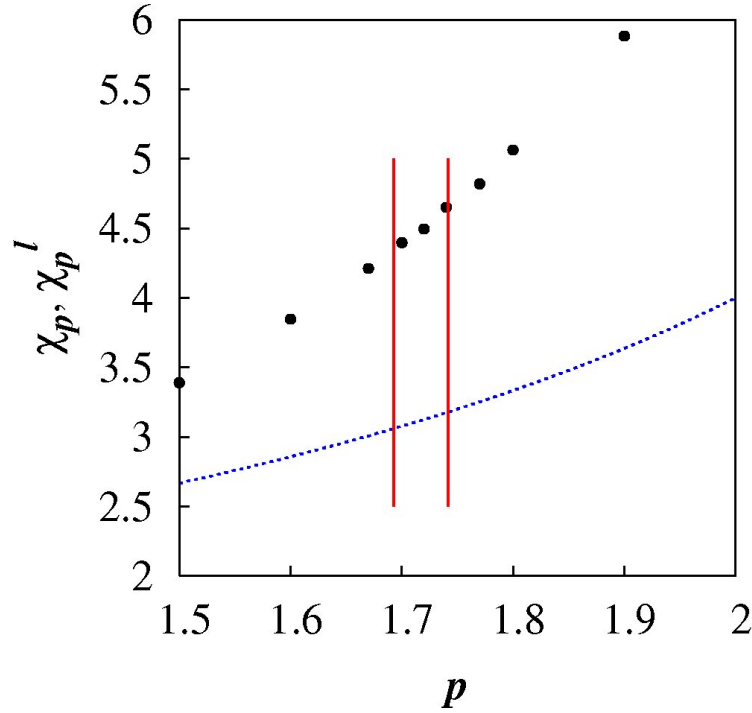


FIGURE 9. χ_p, χ_p^l , against p . Similar to figure 8, but focussing in the range of real turbulence with intermittency. The two vertical red lines are the lower and upper bounds for intermittent turbulence spectra.

An error of around 1% away from $p = 1$ is therefore reasonable. In the limit $p = 3$ there is no detectible error in M_γ from KS to three decimal places (Table 2).

KS is an established method used by many researchers in turbulent diffusion studies, as noted in the earlier references in this paper. However, some researchers, Thomson & Devenish (2005), Nicolleau & Nowakowski (2011), Eyink & Benveniste (2013), have expressed reservations regarding KS which they believe produces incorrect scalings for pair diffusion statistics because of the lack of true dynamical sweeping of the inertial scales eddies by the larger scales. These authors strongly support locality which they believe to be true in reality, and their inference that KS *must* be incorrect is a direct consequence of this thinking. As we are examining the hypothesis of locality itself here, such a presumption cannot be taken as a given. Furthermore, Malik (2015) has shown through an analysis of pairs of trajectories that the quantitative errors in KS due to the sweeping effect is in fact negligible provided that the simulations are carried out in a frame of reference moving with the large scale sweeping flow. The close agreement of KS with the geophysical data in Figure 1 obtained here provides further support for this conclusion.

6. Discussion and conclusions

Richardson pioneered the scientific discipline of turbulent particle pair diffusion, and assumed a locality scaling for the pair diffusivity due to the inclusion of one data-point from a non-turbulent context. Here, the reappraised 1926 data shows an unequivocal non-local scaling for the turbulent pair diffusivity, $K \sim \sigma_l^{1.564}$, Fig. 1. Consequently, the foundations of turbulent pair diffusion theory have been re-examined here in an effort to resolve one of the most important and enduring problems in turbulence.

The main contribution of this investigation is to propose a new non-local theory of turbulent particle pair diffusion based upon the principle that the turbulent pair diffusion process in homogeneous turbulence is governed by both local and non-local diffusional processes. The theory predicts that in turbulence with generalized energy spectra, $E(k) \sim k^{-p}$, over extended inertial subranges, the pair diffusivity scales like, $K(p) \sim \sigma_l^{\gamma_p}$, with $(1+p)/2 < \gamma_p \leq 2$, in the range $1 < p \leq 3$, which is intermediate between the purely local and purely non-local scaling power laws. The reappraised 1926 geophysical data, Fig. 1, Table 1, provides strong support for the new theory.

Additional support comes from a Lagrangian simulation method, KS, whose results for turbulence with intermittency is in remarkably close agreement with the geophysical data in Figure 1, to within 1% error in the scaling power for energy spectra in the accepted range of intermittency; for $E(k) \sim k^{-1.74}$, KS produces, $K_{\mu_I} \sim \sigma_l^{1.570}$, which is an error of just 0.4% in the scaling power. All other predictions of the new theory have also been confirmed using KS. Thus, an important corollary of the present work is that KS is a more accurate Lagrangian simulation method than previously thought.

A detailed mathematical approach has been developed by expressing the pair diffusivity through a Fourier integral decomposition. *a priori* assumptions regarding locality was not made, and this has led to an expression for K as the sum of local and non-local contributions, equation (4.29). A feature of this approach is that it illustrates how various scalings and closure assumptions are inherent in developing any theory for pair diffusion. Such assumptions are always present even in apparently simpler scaling rules, but are often hidden and unstated.

This work also raises questions about previous works. Some DNS in particular have reported pair separation scaling that are close to, $\sim t^3$. How convincing is this in support of a locality hypothesis?

In the first place, Richardson's 1926 data still remains the most comprehensive data on large geophysical scales till now, and it shows unequivocal non-local scaling. It is difficult to reconcile this with the apparent locality scaling reported in some studies, especially in view of the very short inertial subranges that they contain.

Furthermore, fully developed turbulence containing intermittency in a large inertial subrange should not in fact produce a R-O scaling of, $K \sim \sigma_l^{4/3}$, even under the locality hypothesis as we have seen in Section 5.4. The scaling in $\langle l^2 \rangle$ in particular is very sensitive to the power in the energy spectrum through equation (41). With the intermittency observed in real turbulence and under the assumption of locality this would produce a scaling of, $K \sim \sigma_l^{1.35}$ to $\sim \sigma_l^{1.385}$, or equivalently $\langle l^2 \rangle \sim t^{3.077}$ to $\sim t^{3.252}$, which should be detectable if present; but except for Richardson's revised 1926 dataset presented here, no study has reported a scaling greater than $\sim t^3$ strongly indicating that asymptotically large inertial subranges have not yet been achieved in experiments and DNS.

Under the current theory, we would expect even larger scaling powers, asymptoting approximately towards $K_{\mu_I} \sim \sigma_l^{1.57}$ and $\langle l^2 \rangle_{\mu_I} \sim t^{4.65}$.

It is expected that attention will now turn towards the implications of this new theory for the general theory of turbulence, and for turbulence diffusion modeling strategies.

Acknowledgements The author would like to thank SABIC for funding this work through project number SB101011, and the ITC Department at KFUPM for making available the High Performance Computing facility for this project. The author would also like to thank Mr. K. A. K. K. Daoud for producing the parallel version of the KS code. The author has benefitted from useful discussions on this topic with Professor A. Umran Dogan of King Fahd University of Petroleum & Minerals and the University of Iowa.

REFERENCES

- AKERBLOM, F. 1908. *Nova Acta Reg. Soc. Upsaliensis*. (Proc. Roy. Soc.)
- ANSELMET, F., ANTONIA, R. A. & DANAILA, L. 2001 Turbulent flows and intermittency in laboratory experiments. *Planetary and Space Science*, **49**, 11771191.
- BATCHELOR, G. K. 1952 Diffusion in field of Homogeneous Turbulence II. The relative motion of particles. *Math. Proc. Camb. Phil. Soc.* **48** (2), 345–362.
- BATCHELOR, G. K. 1953. *The Theory of Homogeneous Turbulence*. , Cambridge University Press.
- BENZI, R. 2011. A Voyage Through Turbulence. *Eds. P. A. Davidson, Y. Kaneda, H. K. Moffatt, & K. R. Sreenivasan*. **5**, Cambridge University Press.
- BERG, J., LUTHI, B., MANN, J. & OTT, S. 2006 Backwards and forwards relative dispersion in turbulent flow: an experimental investigation. *Phys. Rev. E*, **74**, 016304.
- BERLOFF, P. S., MCWILLIAMS, J. C. & BRACCO, A. 2002 Material Transport in Oceanic Gyres. Part I: Phenomenology *J. Phys. Oceanogr.* **32**, 764–796.
- L. BIFERALE, A.S. LANOTTE, R. SCATAMACCHIA AND F. TOSCHI. 2014 Time scales of turbulent relative dispersion. *J. Fluid Mech.* **757**, 550.
- BITANE R., HOLMAN H. & BEC J. 2012 Time scales of turbulent relative dispersion. *Phys. Rev. E* **86**:045302(R).
- BOFFETTA & CELANI. 2000 Pair dispersion in turbulence.
- BOFFETTA, G. & SOKOLOV, I. M. 2002 Statistics of two-particle dispersion in two-dimensional turbulence. *Phys. Fluids* **14**, 32243232.
- BOURGOIN, M., OUELETTE, N. T., XU, H., BERG, J. & BODENSCHATZ, E. 2006 The role of pair dispersion in turbulent flow. *Science*, **311**, 835838.
- DEFANT, A. 1921. Die Zirkulation der Atmosphre in den gemssigten Breiten der Erde. *Geogaf. Ann.* **3**, 209-266; and Wien. Akad. Wiss. Sitzb. IIa, Vol. 130, 401 (1921).
- EYINK, G. L. & BENVENISTE, D. 2013 Suppression of particle dispersion by sweeping effects in synthetic turbulence. *Phys. Rev. E* **87**, 023011.

- G. FALKOVICH, K. GAWDZKI, AND M. VERGASSOLA 2001 Particles and fields in fluid turbulence. *Rev. Mod. Phys.* **73**, 913.
- M. FARHAN, F. C. G. A. NICOLLEAU, & A. F. NOWAKOWSKI 2001 Effect of gravity on clustering patterns and inertial particle attractors in kinematic simulations. *Phys. Rev. E* **91**, 043021.
- FUNG J. C. H., HUNT J. C. R., MALIK N. A. & PERKINS R. J. 1992 Kinematic simulation of homogeneous turbulence by unsteady random Fourier modes. *J. Fluid Mech.* **236**, 281–318.
- FUNG J. C. H. & VASSILICOS J. C. 1998 Two-particle dispersion in turbulent-like flows. *Phys. Rev. E* **57**, 1677–1690.
- HESELBERG, TH. & SVERDRUP, H. U 1915. *Leipzig Geophys. Inst., Ser. 2*, **Heft 10**.
- HUBER, M., MCWILLIAMS, J. C. & GHIL, A. 2001 A Climatology of Turbulent Dispersion in the Troposphere. *J. Atmos. Sci.* **58**, 22377.
- ISHIHARA, T., GOTOH, T. & KANEDA, Y. 2009 Study of High Reynolds Number Isotropic Turbulence by Direct Numerical Simulation. *Ann. Rev. Fluid Mech.* **41**, 160185.
- ISHIHARA, T. & KANEDA, Y. 2002 Relative diffusion of a pair of fluid particles in the inertial subrange of turbulence. *Phys. Fluids* **14**, L6972.
- JOERGENSEN, J. B., MANN, J., OTT, S., PECSELI, H. L. & TRULSEN 2005 Experimental studies of occupation and transit times in turbulent flows. *Phys. Fluids* **17**, 035111.
- JULIAN, P., MASSMAN, W. & LEVANON, N. 1977 The TWERL experiment. *Bull. Am. Meteorol. Soc.* **58**, 936948.
- M.C. JULLIEN, J. PARET, & P. TABELING. 1999 Richardson pair dispersion in two-dimensional turbulence. *Phys. Rev. Lett.* **82** (14), 2872. *Physica A* **280**, 1-9.
- KAY, G. W. C. & LABY, T. H. 1982. Physical and Chemical Constants I. **Longman**, London.. (Modern Version: G. W. C. Kay and T. H. Laby, Table of Physical and Chemical Constants, Longmans, London, 1982)
- KLAFTER J, BLUMEN A, SHLESINGER MF. 1987 Stochastic pathway to anomalous diffusion. *Phys. Rev. A* **35**, 308185.
- KOLMOGOROV A. N. 1941 The local structure of turbulence in incompressible viscous fluid for very large Reynolds numbers. *Dokl. Akad. Nauk SSSR* **30**(4), 1539. *Translation: Proc. R. Soc. London A* **434**, 9-13, (1991).
- KRAICHNAN, R. H. 1970 Diffusion by a random velocity field. *Phys. Fluids* **13**, 22–31.
- LACASCE, J. H. & OHLMANN, C. 2003 Relative dispersion at the surface of the Gulf of Mexico. *J. Mar. Res.* **61**, 285312.
- LA PORTA, A., VOTH, G. A., CRAWFORD, A. M., ALEXANDER, J. & BODENSCHATZ, E. 2001. Fluid particle accelerations in fully developed turbulence. *Nature* **409**, 1017-1019.
- MAAS, H. G., GRUEN, A. & PAPANTONIOU, D. A. 1993 Particle tracking velocimetry in three-dimensional flows. Part 1. *Exp. in Fluids*, **15**, 133–146.
- MALIK, N. A. 2015 Residual sweeping effect in turbulent pair diffusion in a Lagrangian diffusion model. *PLOS ONE*, *submitted*, <http://arxiv.org/abs/1501.07186v2>.

- MALIK N. A. 1996 Structural diffusion in 2D and 3D random flows. *Adv. in Turb. VI*, 619. Eds. S. Gavrilakis et al. Kluwer Academic Publishers.
- MALIK, N. A., DRACOS, TH. & PAPANTONIOU D. A. 1993 Particle tracking velocimetry in three-dimensional flows. Part 2. *Exp. in Fluids*, **15**, 279–294.
- MALIK N. A. & VASSILICOS J. C. 1999 A Lagrangian model for turbulent dispersion with turbulent-like flow structure: comparison with direct numerical simulation for two-particle statistics. *Phys. Fluids* **11**, 1572–1580.
- MAXEY, M.R. 1987 The gravitational settling of aerosol particles in homogeneous turbulence and random flow fields. *J. Fluid Mech.* **174**, 441–465.
- MENEGUZ, E. & REEKS, M. 2011 Statistical properties of particle segregation in homogeneous isotropic turbulence. *J. J. Fluid Mech.* **686**, 338–351.
- MEYERS, J. & MENEVEAU, C. A. 2008 Functional form for the energy spectrum parametrizing bottleneck and intermittency effects. *Phys. Fluids*, **20**, 065109.
- MOREL, P. & LARCHAVEQUE, M. 1974 Relative Dispersion of Constant-Level Balloons in the 200-mb General Circulation *J. Atm. Sci.* **31**, 2189–2196.
- NICOLLEAU, F. C. G. A. & NOWAKOWSKI, A. F. 2011 Presence of a Richardson's regime in kinematic simulations
- OBUKHOV, A. 1941 Spectral energy distribution in a turbulent flow. *Izv. Akad. Nauk. SSSR. Ser. Geogr. i Geozh* **5**, 453–466. (Translation : Ministry of Supply. p. 21 1097).
- OLLITRAULT M., GABILLET C. & DE VERDIÈRE A. C. 2005 Open ocean regimes of relative dispersion. *J. Fluid Mech.* **533**, 381–407.
- OUELLETTE N. T., XU H., BURGOIN M. & BODENSCHATZ E. 2006. An experimental study of turbulent relative dispersion models. *New J. Phys.* **8**, 109.
- PERKINS, R. J., MALIK, N., A. & FUNG, J. C. H. 1993 Cloud Dispersion Models. *Appld Sci. Res.* **51**, 539–545; *Adv. in Turb. IV*, Kluwer Academic Publishers.
- PERRY, A. E., HENBEST, S., & CHONG, M. S. 2005 A theoretical and experimental study of wall turbulence. *J. Fluid Mech.* **165**, 163–199.
- POPE, S. B. 1994 Lagrangian PDF methods for turbulent flows. *Annu. Rev. Fluid Mech.* **26**, 23–63.
- RICHARDSON, L. F. 1922. Weather Prediction by Numerical Process. *Cambridge University Press.* **p. 221.**
- RICHARDSON L. F. 1926 Atmospheric diffusion shown on a distance-neighbour graph. *Proc. Roy. Soc. Lond. A* **100**, 709–737.
- RICHARDSON, L. F. & PROCTOR, D. 1925. Diffusion over distances ranging from 3 km to 86 km. *Mem. Roy. Meteor. Soc.* **1(1)**, 1–16.
- RICHARDSON L. F. & STOMMEL, H. 1948. Note on Eddy Diffusion in the Sea *J. of Meteorology*, **5**, 238–240.
- SALAZAR, J. P. L. & COLLINS, L. R. 2009 Two-particle dispersion in isotropic turbulent flows. *Annu. Rev. Fluid Mech.* **41**, 405–432.

- SAWFORD B. L., YEUNG P. K. & HACKL J. F. 2008 Reynolds number dependence of relative dispersion statistics in isotropic turbulence. *Phys. Fluids* **20**:065111,
- SCATAMACCHIA, R., BIFERALE, L. & TOSCHI, F. 2012 Extreme events in the dispersion of two neighboring particles under the influence of fluid turbulence. *Phys. Rev. Lett.* **109**:144501.
- SCHMIDT, W. 1917. *Wien. Akad. Sitzb. IIa* **126**, 773. (Notes Rec. Roy. Soc.)
- SHRAIMAN, B. I. & SIGGIA, E. D. 2000 Scalar turbulence. *nature* **405**, 639–646.
- STOMMEL, H. 1949. Horizontal diffusion due to oceanic turbulence. *J. of Marine Research*, **8**, 199–225.
- SULLIVAN, P. J. 1971 The distance-neighbour function for relative diffusion *J. Fluid Mech.* **47**, 601–607.
- TATARSKI, V. I. 1960 Radiophysical methods for the investigation of atmospheric turbulence. *Izv. Vyssh. Uchebn. Zaved. 3 Radiofizika* **4**, 551583.
- TAYLOR, G. I. 1915. Eddy motion in the atmosphere. *Phil. Trans. Roy. Soc. Lond. A* **215**, 126.
- TENNEKES, H. & LUMLEY, J. L. 1972 A first course in Turbulence. *M. I. T.* .
- THOMSON, D. J. & DEVENISH, B. J. 2005 Particle pair separation in kinematic simulations. *J. Fluid Mech.* **526**, 277–302.
- TSUJI, Y. 2004 Intermittency effect on energy spectrum in high-Reynolds number turbulence. *Phys. Fluids*, **16**(5), L43. *Phys. Rev. E* **83**, 056317.
- TSUJI, Y. 2009 High-Reynolds-number experiments: the challenge of understanding universality in turbulence. *Fluid Dyn. Res.*, **41**, 064003.
- TURFUS, C. & HUNT, J.C.R. 1987 A stochastic analysis of the displacements of fluid element in inhomogeneous turbulence using Kraichnans method of random modes. *Adv. in Turb.* Eds. G . Comte-Bellot & J. Mathieu, pp. 191203. Springer.
- VAILLANCOURT, P. A. & YAU, M. K. 2000 Review of particle-turbulence interactions and consequences for cloud physics. *Bull. Am. Meteorol. Soc.* **81**, 285–298.
- WILKINS E. M. 1958 Observations on the separation of pairs of neutral balloons and applications to atmospheric diffusion theory. *J. Meteor.* **17**, 324–327.
- VIRANT, M. & DRACOS, TH. 1997 3D PTV and its application on Lagrangian motion. *Meas. Sci. Technol.* **8**, 1539.
- WOLF, M. C., VOIGT, R. & MOORE, P. A. 2004 Spatial arrangement of odor sources modifies the temporal aspects of crayfish search strategies. *J. Chem. Ecology* **30**(3), 501–517.
- YAO, H.-D. & HE, G.-W. 2009 A kinematic subgrid scale model for large eddy simulation of turbulence-generated sound. *J. of Turbulence*, **10**(19), 114.
- YEUNG, P. K. 1994 Direct numerical simulation of two-particle relative *Phys. Fluids* **6**, 3416–3428.
- YEUNG, P. K. & BORGAS, M. S. 2004 Relative dispersion in isotropic turbulence: Part 1. Direct numerical simulations and Reynolds number dependence. *J. Fluid Mech.* **503**, 93–124.